SRA: A Sensing Radius Adaptation Mechanism for Maximizing Network Lifetime in WSNs

Chao-Tsun Chang, *Member, IEEE*, Chih-Yung Chang, *Member, IEEE*, Shenghui Zhao, Jian-Cheng Chen, and Tzu-Lin Wang

***Abstract*—Coverage is an important issue that has been widely discussed in wireless sensor networks (WSNs). However, it is still a big challenge to achieve both purposes of full coverage and energy balance. This paper considers the area coverage problem for a WSN in which each sensor has a variable sensing radius. To prolong the network lifetime, a weighted Voronoi diagram (WVD) is proposed as a tool for determining the responsible sensing region of each sensor according to the remaining energy in a distributed manner. The proposed mechanism, which is called sensing radius adaptation (SRA), mainly consists of three phases. In the first phase, each sensor and its neighboring nodes cooperatively construct the WVD to identify the responsible monitoring area. In the second phase, each sensor adjusts its sensing radius to reduce the overlapping sensing region such that the purpose of energy conservation can be achieved. In the last phase, the sensor with the least remaining energy further adjusts its sensing radius with its neighbor for to maximize the network lifetime. Performance evaluation and analysis reveal that the proposed SRA mechanism outperforms the existing studies in terms of the network lifetime and the degree of energy balance.**

***Index Terms*—Area coverage, energy balance, variable sensing radius, weighted Voronoi diagram (WVD), wireless sensor networks (WSNs).**

I. Introduction

Wireless sensor networks (WSNs) have many potential applications, including environmental monitoring, tracking, precision agriculture, military surveillance, smart homes, and so on [1]–[4]. The coverage problem is one of the most important issues in WSNs and has been widely discussed. The coverage problem can be roughly classified into types of area, barrier, and target coverage problems. The area coverage asks each point in a given area to be covered by at least one sensor [5]–[7], whereas the barrier coverage aims at using the minimal number of sensors to construct a barrier for detecting intruders crossing the given strip area [8], [9]. Different from area and barrier coverage problems, the target coverage problem only concerns some certain points in the monitoring region and aims to monitor these points by a set of active sensors [10]–[12].

In literature, the area coverage issue has attracted much attention. Most studies [13]–[16] developed coverage approaches aiming to detect the coverage holes and then cover the hole for the purpose of full coverage. In [13], the concept of Voronoi diagram is proposed, which helps each sensor to locally discover the coverage hole within its Voronoi cell. The full-coverage purpose can be reached if the sensing range of each sensor fully covered the corresponding Voronoi cell. However, the work in [13] did not consider the energy-unbalanced problem in WSNs where the remaining energies of the sensors are not identical. If it is the case, a part of the sensors will exhaust their energies prior to the others, reducing the surveillance quality of the WSN.

The work in [14] considered the area coverage problem for a heterogeneous WSN, where each sensor has an adjustable sensing radius. To achieve the full-coverage purpose, a Voronoi–Laguerre diagram technique is proposed in [14], which defines a specific Laguerre distance for each sensor to locally determine the size of its responsible sensing region. Then, to conserve the limited energy, each sensor adjusts its sensing radius according to the size of its own sensing region. However, the calculation of Laguerre distance does not take into account the factor of the remaining energy of each sensor. That is, the sensor with the lower remaining energy might be responsible for a large sensing region, which should be covered by the one with higher remaining energy. As a result, similar to [13], a part of the sensors with lower remaining energies might exhaust their energies earlier than the others; thus, the coverage hole might appear.

To balance the energy consumptions of all sensors, some other studies [15], [16] deployed specific sensors whose sensing radii are adjustable. In [15] and [16], Delaunay triangles are constructed for every three adjacent sensors located in the monitoring region. For each Delaunay triangle, the three sensors will derive the centroid of the triangle, and then, the three sensors adjust their sensing radii to exactly cover the derived centroid. Nevertheless, consider a case shown in Fig. 1. The notation $\Delta s_a s_b s_c$ is a Delaunay triangle formed by sensors s_a, s_b, and s_c. The notations m_a, m_b, and m_c denote the remaining energies of sensors s_a, s_b, and s_c, respectively. In

Manuscript received March 13, 2014; revised December 14, 2015; accepted January 20, 2016. Date of publication January 27, 2016; date of current version December 14, 2016. This work was supported in part by the Ministry of Science and Technology of Taiwan under Contract MOST 104-2221-E-164-003 and in part by the National Natural Science Foundation of China under Award 61472057. The review of this paper was coordinated by Prof. L. Guo. *(Corresponding author: Chih-Yung Chang.)*

C.-T. Chang is with the Department of Information Management, Hsiuping University of Science and Technology, Taichung 41280, Taiwan (e-mail: cctas@mail.hust.edu.tw).

C.-Y. Chang and J.-C. Chen are with the Department of Computer Science and Information Engineering, Tamkang University, New Taipei City 25137, Taiwan (e-mail: cychang@mail.tku.edu.tw; kkperson@gms.tku.edu.tw).

S. Zhao is with the School of Computer and Information Engineering, Chuzhou University, Anhui 239000, China (e-mail: shzhao@ah.edu.cn).

T.-L. Wang is with the Information and Communications Research Laboratories, Industrial Technology Research Institute, Hsinchu 31040, Taiwan (e-mail: LinziWang@itri.org.tw).

Color versions of one or more of the figures in this paper are available online at http://ieeexplore.ieee.org.

Digital Object Identifier 10.1109/TVT.2016.2522645

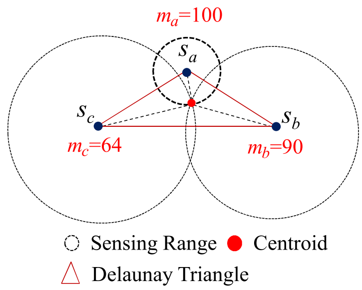

Fig. 1. In this case, the sensing radius of s_a is the shortest even if s_a has the maximal remaining energy.

this case, $\Delta s_a s_b s_c$ is an obtuse angle. Consider that sensor s_a has the maximal remaining energy as compared with s_b and s_c. In Fig. 1, sensor s_a has the maximal remaining energy but contributes the smallest sensing coverage. As a result, sensors s_b and s_c will run out of their energies prior to sensor s_a, reducing the network lifetime.

This paper proposes a sensing radius adaptation (SRA) mechanism that considers the area coverage problem for a WSN where each sensor has variable sensing radius. A weighted Voronoi diagram (WVD) is proposed as a tool for determining the responsible sensing region of each sensor according to its remaining energy in a distributed manner. In addition, to maximize the network lifetime, techniques to balance the energy consumption of all sensors are further presented. The main contributions of this paper are itemized as follows.

1) ***Proposing WVD***. The proposed WVD is a novel partition scheme for each sensor to determine the responsible sensing region according to its remaining energy and substantially adjusts its sensing range to exactly cover its responsible sensing region.
2) ***Resolving orphan region (O-Region) problem***. Applying the proposed WVD might raise the O-Region problem in which a sensing hole might be created. This paper proposed a region expansion process (REP) scheme to resolve the O-Region problem.
3) ***Prolonging network lifetime of WSNs***. In the proposed SRA mechanism, each sensor applies the proposed WVD and REP schemes to adjust the sensing range in a distributed manner, achieving the goals of prolonging network lifetime and full coverage.

The remaining part of this paper is organized as follows. Section II gives the network environment and problem formulation of our approach, whereas Section III presents the details of the proposed SRA mechanism. Section IV depicts the algorithm of the proposed SRA mechanism. The performance analysis and simulation of the proposed SRA mechanism are given in Sections V and VI, respectively. Finally, the conclusions of this paper are presented in Section VII.

II. Network Environment and Problem Formulation

Here, the network environment and the assumptions of the given WSN are presented. Then, the problem formulation of the investigated issue is proposed.

A. Network Environment

This paper assumes that a set of n static sensors $S = \{s_1, s_2, \ldots, s_n\}$ are randomly deployed in the monitoring region M. The radius of each sensor is adjustable. Let r_i denote the sensing radius of sensor s_i, and it can only be adjusted to $r^{\max}$ at maximum. The maximum sensing range of all sensors can fully cover the monitoring region M. All sensors in M are aware of their own location information by applying the existing localization schemes [17]–[20]. In addition, each sensor also knows its own and its neighbors' location information and remaining energies by exchanging the *Hello* message with each other.

B. Problem Formulation

This paper considers the area coverage problem for a given WSN where each sensor has variable sensing radius. There are two major objectives in this paper. One is to balance the lifetimes of all sensors, and the other is to minimize the intersection area of any two neighboring nodes.

Equation (1) depicts the goal of this paper, which aims to balance the energy consumptions of all sensors such that their energies can be exhausted almost at the same time. Let sensor s_i have lifetime t_i if it uses r_i as its sensing radius until it exhausts its whole remaining energy. To balance the lifetimes of all sensors, in the following, a lifetime-balanced index F, which is defined according to Jain's fairness index [21], is used to measure the degree of lifetime balancing:

$$\text{Minimal}(F),\ \text{where } F = 1 - \left(\left(\sum_{\forall s_i, \in S} (t_i) \right)^2 \Big/ n \times \sum_{\forall s_i \in S} (t_i)^2 \right). \tag{1}$$

The value of F of a coverage mechanism approaching to 0 indicates that the mechanism provides better fairness in terms of the energy consumption. In addition, to avoid coverage redundancy, the following gives the secondary goal of this paper. Let o_i denote the sensing region of sensor s_i and y_{ij} denote the area size of intersection region of sensors s_i's and s_j's sensing regions. Therefore, we have

$$y_{ij} = |o_i \cap o_j|,\ \text{where } |a| \text{ denotes the size of region } a. \tag{2}$$

Let R denote the total overlapping area of all deployed sensors. The intersection area of any two neighboring nodes should be small to reduce the coverage redundancy. The secondary goal of this paper is presented as follows:

$$\text{Minimal}(R),\ \text{where } R = \sum_{i=1}^{n-1} \sum_{j=i+1}^{n} y_{ij}\ \forall s_i, s_j \in S. \tag{3}$$

The following represents the constraint to satisfy the requirement of full coverage:

$$\bigcup_{\forall s_i \in S} o_i \supseteq M. \tag{4}$$

TABLE I
NOTATIONS USED IN THIS PAPER

Notation	Definition
$S = \{s_1, s_2, \ldots, s_n\}$	S denotes set of n sensor sets
$N(s_i)$	Neighbors of sensor s_i
m_i	Remaining energy of s_i
t_i	Lifetime of sensor s_i
R	Total overlapping area
o_i	Sensing region of sensor s_i
r_i	Sensing radius of sensor s_i
e_i	Energy consumption for a time unit for s_i
$loc(s_i)$	Location of sensor s_i
$dis(x, y)$	Distance between x and y
V_i	The set of Voronoi vertices of sensor s_i
c_i	Voronoi cell of sensor s_i
l_{ij}	Voronoi edge of sensors s_i and s_j
p_{ijk}^{d}	A division point of sensors s_i, s_j, and s_k
v_i^{far}	The farthest Voronoi vertex of sensor s_i
w_i	Sensing workload of sensor s_i
u_i	Sensing circle of sensor s_i
D_i	The set of vertices that should be covered by sensor s_i
$T(s_{least})$	The set of t_j, where $s_j \in N(s_i)$
$\hat{t}$	The least lifetime in set $T(s_{least})$

The given coverage constraint asks that each location of M should be covered by at least one sensor.

III. SENSING RADIUS ADAPTATION MECHANISM

Here, the details of the proposed SRA mechanism are presented. At the conceptual level, the proposed SRA mechanism mainly consists of three phases: WVD construction (WVD-C) phase, overlapping reduction (OR) phase, and improvement on network lifetime (INL) phase. In the WVD-C phase, each sensor locally determines its own responsible sensing region according to its remaining energy. This phase aims to achieve the first goal, as given in (1). Then, in the OR phase, each sensor adjusts its sensing radius to minimize the coverage redundancy and hence achieves the goal as given in (3). Finally, the INL phase aims to prolong the network lifetime by adjusting the sensing radii of some sensors to prolong the lifetime of the sensor with minimal remaining energy. The following presents the proposed WVD-C, OR, and INL phases. To achieve the readability, Table I lists the notations used in this paper.

A. *Weighted Voronoi Diagram Construction Phase*

The WVD-C phase is mainly consisted of the region partition process (RPP) and the REP. The RPP aims to construct a weighted Voronoi cell (WVC) for each sensor. However, the constructed neighboring Voronoi cell might remain as the hole that cannot be covered by any sensor and hence raise the O-Region problem. In the REP, the Voronoi neighbors further cooperatively enlarge their sensing radii to cope with the O-Region problem.

1) Region Partition Process: Recall that the notations r_i and e_i denote the sensing radius of sensor s_i and corresponding

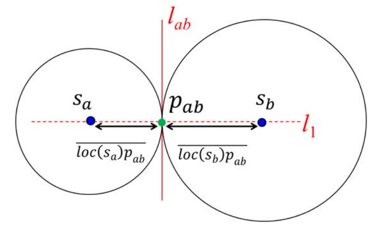

Fig. 2. Sensors s_a and s_b determine their sensing radii based on the line l_{ab}.

energy consumption for a time unit, respectively. According to studies [15], [22], [23], the relation of e_i and r_i can be represented by applying the following:

$$e_i = kr_i^2 \tag{5}$$

where k is a constant.

Let m_i be the remaining energy of sensor s_i. The lifetime t_i of sensor s_i can be measured by the following expression:

$$t_i = \frac{m_i}{kr_i^2}.$$

The following equation asks to balance the lifetime, e.g., t_{ij}, of any two sensors s_i and s_j, i.e.,

$$\frac{m_i}{kr_i^2} = \frac{m_j}{kr_j^2} = t_{ij}. \tag{6}$$

Substituting m_i into (5), the sensing radius of sensor s_i can be derived as follows:

$$r_i = \sqrt{m_i \times \frac{1}{kt_{ij}}}. \tag{7}$$

The proposed SRA algorithm is a greedy algorithm, which makes decisions based on the current remaining energies of any two sensors, s_i and s_j, for balancing their energies. To reach the goal as depicted in (1), sensor s_i and each of its neighbors apply (7) to determine their sensing radii to construct the WVD. The following presents how to construct the WVD.

As shown in Fig. 2, consider two neighboring sensors s_a and s_b. Let notations $loc(s_a)$ and $loc(s_b)$ denote the locations of sensors s_a and s_b. In Fig. 2, there are two lines l_1 and l_{ab} that are perpendicular to one another. Line l_1 is a straight line passing through $loc(s_a)$ and $loc(s_b)$, whereas l_{ab} is the sensing boundary that s_a and s_b desire to calculate. Let p represent the intersection point of lines l_1 and l_{ab}. As shown in Fig. 2, sensing boundary l_{ab} partitions line l_1 into two segments: $\overline{loc(s_a)p_{ab}}$ and $\overline{loc(s_b)p_{ab}}$. Let r_a and r_b denote the desired sensing radii that cause sensors s_a and s_b to have identical lifetimes. To achieve the goal given in (1) such that the lifetimes of sensors s_a and s_b are identical, (7) is locally applied by sensors s_a and s_b, aiming to derive the values of r_a and r_b based on their remaining energies. Accordingly, the sensing radii of sensors s_a and s_b can be calculated by

$$r_a = \sqrt{m_a \times \frac{1}{kt_{ab}}} \text{ and } r_b = \sqrt{m_b \times \frac{1}{kt_{ab}}}. \tag{8}$$

Based on (8), sensors s_a and s_b further evaluate the ratio of r_a and r_b, as shown in the following:

$$r_a : r_b = \sqrt{m_a \times \frac{1}{kt_{ab}}} : \sqrt{m_b \times \frac{1}{kt_{ab}}} = \sqrt{m_a} : \sqrt{m_b}. \quad (9)$$

As a result, sensors s_a and s_b calculate the values of $dis(loc(s_a), p_{ab})$ and $dis(loc(s_b), p_{ab})$ according to (10) and (11) in the following to locally determine the location of p_{ab}:

$$dis\,(loc(s_a), p_{ab}) = dis\,(loc(s_a), loc(s_b)) \times \frac{\sqrt{m_a}}{\sqrt{m_a} + \sqrt{m_b}} \quad (10)$$

$$dis\,(loc(s_b), p_{ab}) = dis\,(loc(s_a), loc(s_b)) \times \frac{\sqrt{m_b}}{\sqrt{m_a} + \sqrt{m_b}}. \quad (11)$$

To ease the presentation of WVD, the following defines the terms of weighted partition point, weighted Voronoi edge, and WVC. The point p determined by applying (10) and (11) is referred to as weighted partition point of sensors s_a and s_b. The line l_{ab} is referred to as weighted Voronoi edge of sensors s_a and s_b. Any two nonparallel weighted Voronoi edges of sensor s_a will intersect at a point called weighted Voronoi vertex. Each weighted Voronoi vertex of sensor s_a can determine responsible sensing region for sensor s_a. Let c_i denote the WVC of sensor s_i and V_i denote the Voronoi vertex set of cell c_i. To achieve the purpose of full coverage, sensor s_i should fully cover all its vertices. Based on the WVC constructed by each sensor, the WVD can be constructed. In addition, the boundary of the monitoring area is also considered in the WVD-C phase. Any node located near the boundary should treat the boundary as the weighted Voronoi edge of its Voronoi cell to avoid creating the coverage hole. The following gives the formal definition of WVD.

Definition 1—Weighted Voronoi Diagram WVD(V, E): Given a deployed WSN containing a set of sensors $S = \{s_1, s_2, s_3, \ldots, s_n\}$. Each sensor has constructed its Voronoi cell by RPP. Let V and E denote the vertex set of all weighted Voronoi vertices of a cell and the edge set of all weighted Voronoi edges of a cell, respectively. A WVD of S, denoted by WVD(V, E), which consists of a vertex set V and an edge set E. □

The following gives an example to illustrate how the sensor applies the RPP to construct its WVC. As shown in Fig. 3, sensor s_a has five neighbors, and it intends to establish its WVC. We take the sensors s_a and s_e as an example to illustrate how they determine the weighted partition point p_{ae}. The remaining energies of sensors s_a and s_e are 64 and 36, respectively. By applying (9), sensors s_a and s_e have the following calculation:

$$r_a : r_e = \sqrt{m_a} : \sqrt{m_b} = 4 : 3.$$

Based on this ratio, sensor s_a can derive its sensing radius by applying (10) and (11) as follows:

$$dis\,(\mathrm{loc}(s_a), p_{ae}) = dis\,(\mathrm{loc}(s_a), \mathrm{loc}(s_e)) \times \frac{4}{4+3}.$$

As a result, the weighted Voronoi edge l_{ae} can be established. Similarly, sensor s_a establishes all the other weighted Voronoi edges with its neighbors' locations. As shown in Fig. 3, by executing RPP, the WVC c_a will be constructed; hence, we have $V_a = \{v_a^1, v_a^2, v_a^3, v_a^4, v_a^5\}$. Once sensors s_a fully covers its WVC, it terminates the RPP.

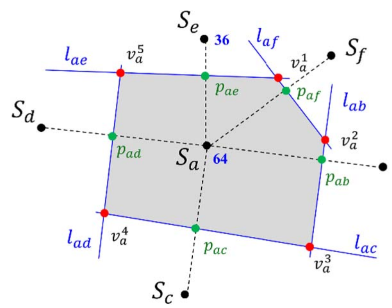

Fig. 3. Each sensor applies the proposed RPP to locally determine its WVC (responsible sensing region).

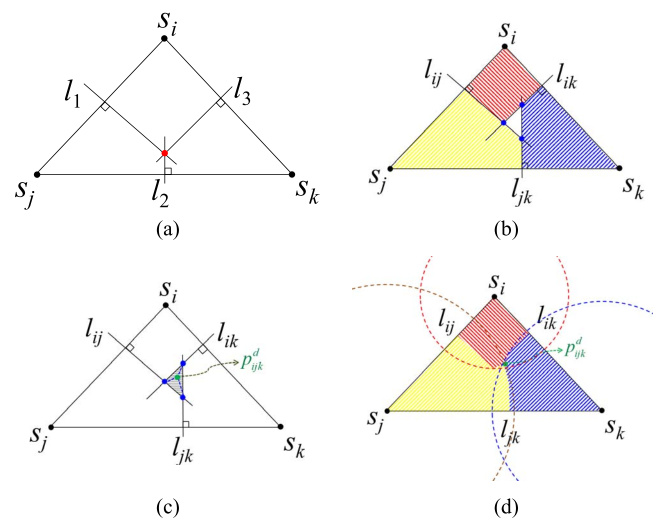

Fig. 4. In the OR phase, the sensors apply the REP to cooperatively cover the O-region. (a) By applying traditional VD, three lines l_1, l_2, and l_3 will intersect at circumcenter without creating any hole. (b) Central triangular region cannot be covered by sensors s_i, s_j, and s_k after applying RPP. (c) By applying REP, a division point p_{ijk}^d is selected to connect three blue points. (d) After applying REP, the uncovered region can be cooperatively covered by sensors s_i, s_j, and s_k.

2) Region Expansion Process: The constructed WVD is different from the traditional Voronoi diagram (VD) [13]. In the traditional VD, the monitoring region is fully covered if every sensor can fully cover its Voronoi cell. However, the constructed WVD does not guarantee that the monitoring region is fully covered, although each sensor adjusts its sensing radius to fully cover its Voronoi cell. The problem of existing hole refers to the orphan problem. The following gives Fig. 4 to illustrate the difference between constructed WVD and traditional VD and shows the orphan problem.

As shown in Fig. 4(a), three neighboring sensors s_i, s_j, and s_k apply the traditional VD construction approach [13] to determine their Voronoi edges. In Fig. 4(a), lines l_1, l_2, and l_3 equally bisect segments $\overline{loc(s_i)loc(s_j)}$, $\overline{loc(s_j)loc(s_k)}$, and $\overline{loc(s_l)loc(s_k)}$, respectively. Hence, lines l_1, l_2, and l_3 must intersect at a point known as the circumcenter. On the other hand, as shown in Fig. 4(b), by applying the proposed RPP, the three edges l_{ij}, l_{jk}, and l_{ik} cannot intersect at one point. As a result, the central triangular region might be a hole that raises the O-Region problem, as formally defined in the following.

O-Region Problem: Consider three neighboring sensors s_i, s_j, and s_k, as shown in Fig. 4(b). The three weighted Voronoi edges l_{ij}, l_{jk}, and l_{ik} might form a specific orphan region that is not fully covered even if each sensor fully covers its Voronoi cell. The existence of triangular hole refers to the O-Region problem. □

Here, we further propose the REP to cope with the O-Region problem. The basic concept behind the proposed REP is to determine a division point, denoted by p^d_{ijk}, in the O-Region, as shown in Fig. 4(c). When sensors incur O-Region problem, they will adjust their sensing radii to cover the division point p^d_{ijk} such that the O-Region can be fully covered. To balance the remaining energies of those sensors that incur the O-Region problem, the following depicts the properties that should be satisfied for determining a good division point p^d_{ijk}.

Constraints of Division Point (p^d_{ijk}): Consider that sensors s_i, s_j, and s_k incur the O-Region problem. A division point, denoted by p^d_{ijk}, in the O-Region should satisfy the following two criteria.

Criterion 1: It is located inside the O-Region.
Criterion 2: $|\overline{s_l p}| : |\overline{s_j p}| : |\overline{s_k p}| = \sqrt{m_i} : \sqrt{m_j} : \sqrt{m_k}$.

□

As shown in Fig. 4(b), sensors s_i, s_j, and s_k incur the O-Region problem where the O-Region is depicted (marked by the white triangular region). Inside the O-Region, a division point p^d_{ijk} will be selected that satisfies criteria 1 and 2. According to criterion 2, the lengths of lines $\overline{s_l p^d_{ljk}}$, $\overline{s_j p^d_{ljk}}$, and $\overline{s_k p^d_{ljk}}$ can be presented as $\sqrt{m_i}x$, $\sqrt{m_j}x$, and $\sqrt{m_k}x$, respectively, where x is a constant. The following expression depicts that the size of area $\Delta s_i s_j s_k$ can be calculated by using the edge length.

$$\text{area}(\Delta s_i s_j s_k) = \sqrt{S(S - \overline{s_l s_k})(S - \overline{s_l s_j})(S - \overline{s_j s_k})},$$

where $S = (\overline{s_l s_j} + \overline{s_l s_k} + \overline{s_j s_k})/2$.

Since $\Delta s_i s_j s_k$ can be divided into three triangle regions, $\Delta s_i s_j p^d_{ijk}$, $\Delta s_i p^d_{ijk} s_k$, and $\Delta p^d_{ijk} s_j s_k$, the size of area $\Delta s_i s_j s_k$ equals to the summation of areas $\Delta s_i s_j p^d_{ijk}$, $\Delta s_i p^d_{ijk} s_k$, and $\Delta s_i s_j p^d_{ijk}$, $\Delta p^d_{ijk} s_j s_k$. By substituting the value of constant x, the lengths of lines $\overline{s_l p^d_{ljk}}$, $\overline{s_j p^d_{ljk}}$, and $\overline{s_k p^d_{ljk}}$ are obtained; thus, the sensing radii of sensors s_i, s_j, and s_k are derived. To handle O-Region problem, point p^d_{ijk} should be the common vertex that the sensors s_i, s_j, and s_k should adjust their sensing radii to cover the point. After applying REP, the O-Region problem is eliminated, as shown in Fig. 4(d).

B. *Overlapping Reduction Phase*

After the execution of WVD-C phase, all sensors can locally determine their own WVCs, and the monitoring region will be fully covered. However, the coverage redundancy might be large since each sensor locally executes the proposed RPP and REP (if any). This subsection further proposes an OR phase aiming at reducing the coverage redundancy to satisfy the goal given in (3), whereas the full coverage constraint should be satisfied. To ease the presentation, the following gives the definition that is used in the OR phase. Let $v_i^{\text{far}} \in V_i$ denote the farthest vertex away from location of sensor s_i. Definition 2 defines fixed node and adjustable node.

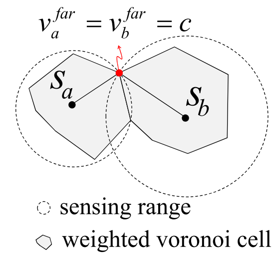

Fig. 5. Sensors s_a and s_b are fixed nodes. That is, if either s_a or s_b reduces its sensing radius, it will raise a coverage hole.

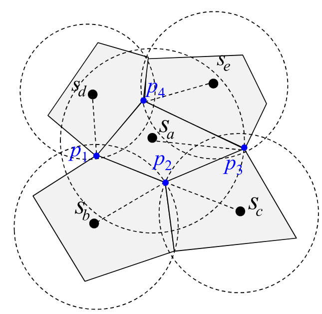

Fig. 6. Sensor s_a is an adjustable node and applies the OR phase.

Definition 2—Fixed Node and Adjustable Node: A sensor, e.g., s_i, is referred to as fixed node if there exists a neighboring node s_j satisfying the condition $v_i^{\text{far}} = v_j^{\text{far}}$. Otherwise, it is called adjustable node. □

A fixed node, e.g., s_i, cannot locally reduce its sensing radius because the reduction of its sensing radius cannot cover the Voronoi vertex v_i^{far}. As shown in Fig. 5, consider two neighboring sensors s_a and s_b. Assume that $v_a^{\text{far}} = v_b^{\text{far}} = c$. If sensor s_a (or s_b) reduces its sensing radius, a coverage hole will be created.

The following gives an overview to illustrate the proposed OR phase.

1) Overview of OR Phase: In the OR phase, each sensor locally verifies if it is an adjustable node. If it is the case, the sensor can execute the OR phase for reducing its sensing radius. The OR phase mainly consists of reconstructing WVC based on a fixed node (RFN), reconstructing WVC based on an adjustable node (RAN), and sensing radius evaluation (SRE) tasks. In the RFN task, each sensor that neighbors to the fixed node will try to replace its Voronoi vertices by the other closer vertices. This action can reduce the size of the Voronoi cell such that the sensor can conserve its energy while the full coverage property is still maintained. In the RAN task, the adjustable node that has higher workload than the other adjustable nodes can further reduce its sensing radius by replacing its weighted Voronoi vertices with the other closer vertices. In the SRE task, the adjustable node evaluates its new sensing radius based on the vertex set determined in the RFN and RAN tasks.

The following gives an example, from Figs. 6–9, to illustrate the concepts of the three tasks. As shown in Fig. 6, assume that

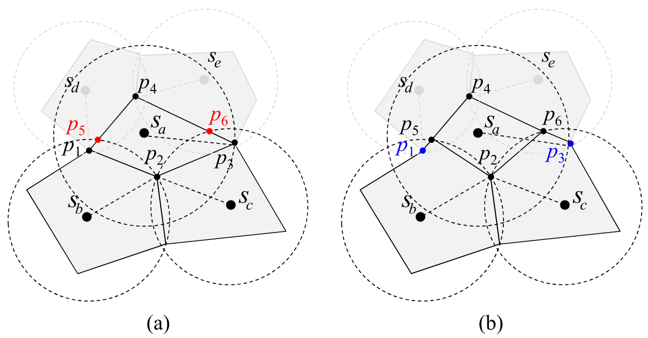

Fig. 7. Sensor s_a executes the RFN task to determine the new weighted Voronoi edges between its neighboring fixed nodes and itself. (a) Initial WVC of s_a. (b) New WVC for s_a.

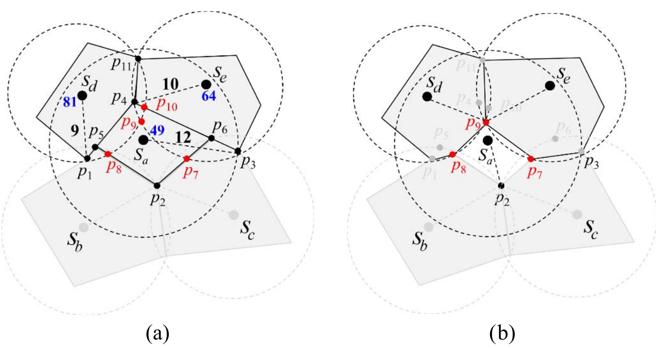

Fig. 8. By executing the RAN task, sensor s_a can determine its new weighted Voronoi vertex cell. (a) Sensor s_a executes RAN task and hence set $V_a = p_2, p_4, p_5, p_6, p_7, p_8, p_9, p_{10}$ is obtained. (b) Sensor s_a removes redundant points from set V_a and hence new set $V_a = p_2, p_7, p_8, p_9$ is obtained.

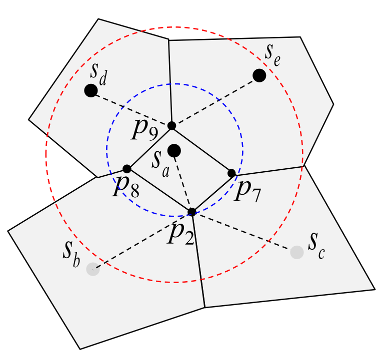

Fig. 9. By applying OR phase, the weighted Voronoi cells of s_a, s_b, s_c, s_d and s_e can be reconstructed.

sensors s_a, s_d, and s_e are adjustable nodes and sensors s_b and s_c are fixed nodes. Sensors s_b and s_c will not execute the OR phase since they are fixed nodes. On the contrary, since sensor s_a neighbors to the fixed nodes, it will execute RFN task. First, sensor s_a checks which Voronoi vertices located within the sensing radii of fixed nodes s_b and s_c. In this case, vertices p_1 and p_3 are located within the sensing radii of fixed nodes s_b and s_c, respectively. In this task, sensor s_a intends to find the other closer vertices to replace vertices p_1 and p_3. Fig. 7(a) further depicts how sensor s_a replaces vertices p_1 and p_3 by the other two points.

As shown in Fig. 7(a), the sensing circles of sensors s_b and s_c intersect with the weighted Voronoi edges l_{ad} and l_{ae} at the points p_5 and p_6, respectively. Therefore, the point p_3 can be replaced by point p_6 since the edge $\overline{p_3p_6}$ is covered by fixed node s_c. Similarly, the point p_1 can also be replaced by point p_5 because the edge $\overline{p_1p_5}$ is covered by fixed node s_b. Consequently, the weighted Voronoi edges $\overline{p_1p_2}$ and $\overline{p_2p_3}$ can be replaced by edges $\overline{p_2p_5}$ and $\overline{p_2p_6}$, respectively, as shown in Fig. 7(b). After executing the RFN task, sensor s_a removes the points p_1 and p_3 from set V_a and adds points p_5 and p_6 in set V_a. Consequently, set $V_a = \{p_2, p_4, p_5, p_6\}$.

After executing RFN task, sensor s_a will execute RAN task that aims to further reduce the size of c_a. The following presents how the sensor s_a executes the RAN task. In the RAN task, sensor s_a applies (5) to calculate the sensing workloads of its neighboring nodes and itself. The sensing workload w_i of each node s_i can be measured by $w_i = kr^2$, where r is the minimal sensing radius that is able to cover the farthest weighted Voronoi vertex of its WVC. As shown in Fig. 8(a), assume that the sensing radii of sensors s_a, s_d, and s_e are 12, 9, and 10, respectively. The remaining energies of sensors s_a, s_d, and s_e are 49, 81, and 64, respectively. The workloads of these sensors can be evaluated, as shown in

$$w_a = k \times 12^2, w_d = k \times 9^2, w_e = k \times 10^2. \tag{12}$$

In this case, sensor s_a has a higher workload than sensors s_d and s_e; it can reduce the size of c_a prior than the other two nodes. In Fig. 8(a), sensor s_a finds those vertices that are intersection points of its Voronoi edges and the sensing circles of its neighboring nodes. These vertices will be verified if they can replace sensor s_a's weighted Voronoi points p_4, p_5, and p_6. To accomplish this, sensor s_a first finds points p_8 and p_{10}, which are the intersection points of the sensing circle of s_d and edges $\overline{p_2p_5}$ and $\overline{p_4p_6}$, respectively. In addition, the sensing circle of adjustable node s_e intersects with edge $\overline{p_2p_6}$ at point p_7. Moreover, two sensing circles of nodes s_d and s_e intersect with each other at point p_9. Since the edge $\overline{p_5p_8}$ can be covered by node s_d, sensor s_a replaces point p_5 by p_8 for reconstructing its WVC without creating any hole. On the other hand, node s_a replaces point p_6 by p_7; hence the weighted Voronoi edge $\overline{p_4p_6}$ of sensors s_a is replaced by edges $\overline{p_4p_9}$ and $\overline{p_7p_9}$. Similarly, the weighted Voronoi edge $\overline{p_4p_5}$ is also replaced by edges $\overline{p_4p_9}$ and $\overline{p_8p_9}$. After executing the RAN task, all the intersection points p_7, p_8, p_9, and p_{10} will be added in the new set V_a to reconstruct the cell c_a. The set V_a is given as follows:

$$V_a = \{p_2, p_4, p_5, p_6, p_7, p_8, p_9, p_{10}\}.$$

Since some points in set V_a can be covered by other adjustable nodes, those points should be removed from V_a. As shown in Fig. 8(b), sensor s_a removes the points p_4, p_5, p_6, and p_{10} from set V_a. The reason is that the points p_4, p_5, p_6, and p_{10} are covered by at least one sensor node. Therefore, set $V_a = \{p_2, p_7, p_8, p_9\}$. In *SRE* task, sensor s_a evaluates which sensing radius is better to cover all points in set V_a. In Fig. 8(b), since point p_2 has the farthest distance between s_a and itself, sensor s_a can further reduce its sensing radius until its sensing radius reached the point p_2. Fig. 9 gives the final weighted Voronoi cell of sensor s_a. The red and blue circles denote the original and adjusted sensing radii of sensor s_a, respectively. This example depicts the concept that the adjustable node s_a

can release its constraint for covering those Voronoi vertices which have been covered by some other fixed and adjustable nodes.

The following formally presents the design of *OR* phase. Let sensor s_k be an adjustable node and some of its neighboring node $s_i^{\text{fixed}} \in N(s_k)$ is a fixed node and the other node $s_j^{\text{adj}} \in N(s_k)$ is an adjustable node. By executing three tasks, sensor s_k can reduce its sensing radius without creating any hole. Section III-B2–III-B4 formally present the RFN, RAN, and SRE tasks, respectively.

2) RFN Task: In this task, as an adjustable sensor s_k neighboring to at least one fixed node aims to decide the new weighted Voronoi edge between its neighboring fixed node $s_i^{\text{fixed}} \in N(s_k)$ and itself. Let u_k denote the sensing circle of sensor s_k. Let u_i^{fixed} and u_j^{adj} denote the sensing circles of fixed sensor s_i^{fixed} and adjustable sensor s_j^{adj}, respectively. The sets $U^{\text{fixed}}(s_k)$ and $U^{\text{adj}}(s_k)$ can be presented as follows:

$$U^{\text{fixed}}(s_k) = \left\{ u_i^{\text{fixed}} \middle| \, s_i^{\text{fixed}} \in N(s_k) \right\}$$
$$U^{\text{adj}}(s_k) = \left\{ u_j^{\text{adj}} \middle| \, s_j^{\text{adj}} \in N(s_k) \right\}.$$

Let v_k^{fixed} denote the weighted Voronoi vertex of sensor s_k that is covered by at least one fixed node and V_k^{fixed} denote the set of v_k^{fixed}. Let $E(s_k)$ denote the set of all weighted Voronoi edges of sensor s_k. Let e_k^{fixed} denote sensor s_k's weighted Voronoi edge, which is partial covered by fixed sensor $s_i^{\text{fixed}} \in N(s_k)$, and E_k^{fixed} be the set of e_k^{fixed}, i.e.,

$$E_k^{\text{fixed}} = \left\{ e_k^{\text{fixed}} \middle| \, e_k^{\text{fixed}} \in E(s_k) \text{ and } e_k^{\text{fixed}} \cap u_i^{\text{fixed}} \neq \emptyset \right\}. \tag{13}$$

In case that set V_k^{fixed} is nonempty, there exists at least one fixed node, e.g., $s_i^{\text{fixed}} \in N(s_k)$, whose sensing circle u_i^{fixed} covers some point $v_k^{\text{fixed}} \in V_k^{\text{fixed}}$. This also indicates that there exists at least one weighted Voronoi edge, e.g., $e_k^{\text{fixed}} \in E(s_k)$, containing the point v_k^{fixed}, which is intersected with the sensing circle u_i^{fixed} at an intersection point. Let $v_{k,w}^{\text{int}}$ denote the intersection point of $u_i^{\text{fixed}} \in U^{\text{fixed}}(s_k)$ and the edge $e_k^{\text{fixed}} \in E_k^{\text{fixed}}$ and $\bar{v}_{k,w'}^{\text{int}}$ denote the intersection points of u_k and the monitoring boundary (if any) and V_k^{int} denote the set of $v_{k,w}^{\text{int}} \cap \bar{v}_{k,w'}^{\text{int}}$. The vertex v_k^{fixed} can be replaced by the wth intersection point $v_{k,w}^{\text{int}}$ since the point $v_{k,w}^{\text{int}}$ is closer to sensor s_k than the vertex v_k^{fixed}. Let $d_{k,q}^{\text{fixed.int}}$ denote the qth intersection point of any two sensing circles $u_i^{\text{fixed}} \in U^{\text{fixed}}(s_k)$ and $u_i^{\text{fixed}'} \in U^{\text{fixed}}(s_k)$ within the cell c_k (in any) and $D_k^{\text{fixed.int}}$ denote the set of $d_{k,q}^{\text{fixed.int}}$. Since the point that belongs to set $V_k^{\text{int}} \cup D_k^{\text{fixed.int}}$ can be covered by at least one sensor, sensor s_k can reduce its sensing radius until its sensing radius reached to the point that belongs to set $V_k^{\text{int}} \cup D_k^{\text{fixed.int}}$ and has the farthest distance to sensor s_k. Based on sets V_k^{int} and $D_k^{\text{fixed.int}}$, sensor s_k can determine its new weighted Voronoi vertex set.

The following formally presents how sensor s_k reconstructs its Voronoi cell for reducing its sensing radius. Let the duty vertices of sensor s_k, denoted by D_k^{org}, be the set of vertices that should be covered by sensor s_k. Before executing the OR phase, we have

$$D_k^{\text{org}} = V_k. \tag{14}$$

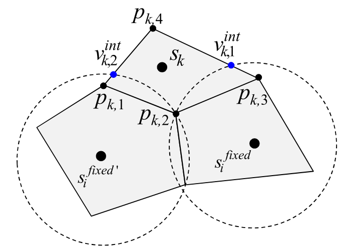

Fig. 10. Set $D_k^{\text{fixed}} = \{v_{k,2}^{\text{int}}, p_{k,2}, v_{k,1}^{\text{int}}, p_{k,4}\}$ can be determined after sensor s_k executes the RFN task. Based on set D_k^{fixed}, sensor s_k further executes the RAN task.

Let D_k^{fixed} denote the set of vertices after sensor s_k executes RFN task. Equation (15) further derives the set D_k^{fixed}. Afterwards, sensor s_k executes the RAN task based on set D_k^{fixed}

$$D_k^{\text{fixed}} = D_k^{\text{org}} - V_k^{\text{fixed}} + V_k^{\text{int}} + D_k^{\text{fixed.int}}. \tag{15}$$

Fig. 10 gives an example to illustrate how sensor s_k reduces its sensing radius by evaluating new set D_k^{fixed} and then reconstructs its WVC. In Fig. 10, the sensing circles $u_i^{\text{fixed}} \in U^{\text{fixed}}(s_k)$ and $u_i^{\text{fixed}'} \in U^{\text{fixed}}(s_k)$ intersect with the edges $\overline{p_{k,3}p_{k,4}} \in E_k^{\text{fixed}}$ and $\overline{p_{k,1}p_{k,4}} \in E_k^{\text{fixed}}$ at points $v_{k,1}^{\text{int}}$ and $v_{k,2}^{\text{int}}$, respectively. That is, sensors s_i^{fixed} and $s_i^{\text{fixed}'}$ are able to cover the edges $\overline{p_{k,3}v_{k,1}^{\text{int}}}$ and $\overline{p_{k,1}v_{k,2}^{\text{int}}}$, respectively. Hence, we have $V_k^{\text{int}} = \{v_{k,1}^{\text{int}}, v_{k,2}^{\text{int}}\}$, $V_k^{\text{fixed}} = \{p_{k,1}, p_{k,2}, p_{k,3}\}$, and $D_k^{\text{fixed.int}} = \{p_{k,2}\}$. By executing the RFN task, set $D_k^{\text{org}} = \{p_{k,1}, p_{k,2}, p_{k,3}, p_{k,4}\}$ can be replaced by set $D_k^{\text{fixed}} = \{v_{k,2}^{\text{int}}, p_{k,2}, v_{k,1}^{\text{int}}, p_{k,4}\}$. As a result, sensor s_k can reduce its sensing radius since points $v_{k,1}^{\text{int}}$ and $v_{k,2}^{\text{int}}$ are closer to sensor s_k than $p_{k,3}$ and $p_{k,1}$, respectively.

3) RAN Task: After executing the RFN task, each adjustable sensor s_k is able to reconstruct its new Voronoi cell based on set D_k^{fixed}. In the RAN task, the adjustable node intends to further reduce its sensing radius by checking if some Voronoi vertices in set D_k^{fixed} can be further replaced by closer points. Since there might exist several adjustable nodes executing the RAN task simultaneously, the adjustable node that has higher workload will have higher priority to execute the RAN task. Each adjustable node s_k calculates its workload w_k and each of its neighbor's workload by applying (5). Let sensor s_k has the highest workload as compared with its neighbors; therefore, it has the highest priority to adjust its sensing radius. Let D_k^{adj} denote the set of vertices after sensor s_k executes the RAN task. Let e_k^{adj} denote the weighted Voronoi edge between the adjustable node $s_j^{\text{adj}} \in N(s_k)$ and sensor s_k, which is partial covered by sensor s_j^{adj}, and notation E_k^{adj} denote the set of e_k^{adj}. Similar to the RFN task, the intersection point of sensing circles of sensors $s_j^{\text{adj}} \in N(s_k)$ and s_k, which is located at e_k^{adj} can be covered by sensor s_j^{adj}. Let $d_{k,j}^{\text{adj}^*}$ denote the ith intersection point of $u_j^{\text{adj}} \in U^{\text{adj}}(s_k)$ and $e_k^{\text{adj}} \in E_k^{\text{adj}}$ and notation $D_k^{\text{adj}^*}$ denote the set of $d_{k,i}^{\text{adj}^*}$. Obviously, the point $d_{k,i}^{\text{adj}^*}$ is closer to the sensor s_k than some point that belongs to set D_k^{fixed}. Let $d_{k,z}^{a.\text{int}}$ denote the intersection points of any two sensing circles u_j^{adj} and $u_j^{\text{adj}'} \in U^{\text{adj}}(s_k)$ within the cell c_k (in any) and notation

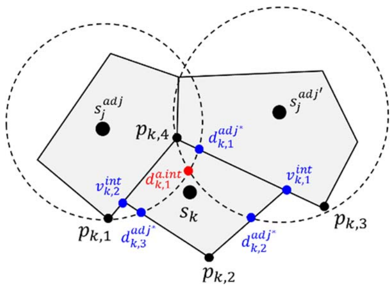

Fig. 11. Sensor s_k obtains the set $D_k^{\text{new}} = \{p_{k,2}, d_{k,2}^{\text{adj}^*}, d_{k,3}^{\text{adj}^*}, d_{k,1}^{a.\text{int}}\}$ by executing the RAN task.

$D_k^{a.\text{int}}$ denote the set of $d_{k,z}^{a.\text{int}}$. Based on sets D_k^{fixed}, $d_k^{\text{adj}^*}$, and $D_k^{a.\text{int}}$, sensor s_k applies (16) to derive the set D_k^{adj} for further reducing its sensing radius

$$D_k^{\text{adj}} = D_k^{\text{fixed}} + D_k^{\text{adj}^*} + D_k^{a.\text{int}}. \tag{16}$$

However, some points might be redundant in set D_k^{adj} since those points can be covered by neighboring adjustable nodes. The sensor s_k should remove some redundant points from set D_k^{adj}. Let D_k^{new} denote the set of weighted Voronoi vertices after sensor s_k applies the RFN and RAN tasks. Let $D_{k,\text{fixed}}^{\text{overlap}}$ and $D_{k,\text{adj}}^{\text{overlap}}$ denote the sets of vertices that should be removed from set D_k^{adj} after sensor s_k executes the RFN and RAN tasks, respectively. The set D_k^{new} can be calculated by applying

$$D_k^{\text{new}} = D_k^{\text{adj}} - D_{k,\text{fixed}}^{\text{overlap}} \cup D_{k,\text{adj}}^{\text{overlap}}. \tag{17}$$

Based on set D_k^{new}, sensor s_k is able to evaluate its sensing radius to conserve further its energy.

Fig. 11 gives an example to illustrate how sensor s_k derives the set D_k^{adj} by executing the RAN task. In Fig. 11, the sensing circle $u_j^{\text{adj}} \in U^{\text{adj}}(s_k)$ intersects with the edge $\overline{p_{k,3}p_{k,4}} \in E_k^{\text{adj}}$ at the point $d_{k,1}^{\text{adj}^*}$ and it also intersects with the edge $\overline{v_{k,2}^{\text{int}}p_{k,2}} \in E_k^{\text{adj}}$ at the point $d_{k,3}^{\text{adj}^*}$. On the other hand, the sensing circle $u_j^{\text{adj}'} \in U^{\text{adj}}(s_k)$ intersects with edge $\overline{v_{k,1}^{\text{int}}p_{k,2}} \in E_k^{\text{adj}}$ at point $d_{k,2}^{\text{adj}^*}$. In addition, two sensing circles u_j^{adj} and $u_j^{\text{adj}'} \in U^{\text{adj}}(s_k)$ intersect at the point $d_{k,1}^{a.\text{int}}$. Therefore, we have

$$D_k^{\text{adj}^*} = \left\{d_{k,1}^{\text{adj}^*}, d_{k,2}^{\text{adj}^*}, d_{k,3}^{\text{adj}^*}\right\} \text{ and } D_k^{a.\text{int}} = \left\{d_{k,1}^{a.\text{int}}\right\}.$$

Recall that the set D_k^{fixed} is obtained by executing RFN task

$$D_k^{\text{fixed}} = \left\{v_{k,2}^{\text{int}}, p_{k,2}, v_{k,1}^{\text{int}}, p_{k,4}\right\}.$$

By executing the RAN task, set D_k^{fixed} will be replaced by set D_k^{adj}, i.e.,

$$D_k^{\text{adj}} = \left\{v_{k,2}^{\text{int}}, p_{k,2}, v_{k,1}^{\text{int}}, p_{k,4}, d_{k,1}^{adj^*}, d_{k,2}^{adj^*}, d_{k,3}^{adj^*}, d_{k,1}^{a.\text{int}}\right\}.$$

In Fig. 11, since we have sets $D_{k,\text{fixed}}^{\text{overlap}} = \{v_{k,1}^{\text{int}}, v_{k,2}^{\text{int}}\}$ and $D_{k,\text{adj}}^{\text{overlap}} = \{p_{k,4}, d_{k,1}^{adj^*}\}$, sensor s_k can derive the set D_k^{new} by applying (17). The set

$$D_k^{\text{new}} = \left\{p_{k,2}, d_{k,2}^{adj^*}, d_{k,3}^{\text{adj}^*}, d_{k,1}^{a.\text{int}}\right\}.$$

Consequently, the adjustable sensor s_k obtains its newly constructed set D_k^{new}.

After executing the RAN task, the adjustable node s_k changes its Voronoi vertex set from set D_k^{org} to the set D_k^{new} and then executes the next task, called SRE task.

4) SRE Task: Let d_k^{far} be the farthest Voronoi vertex of s_k in set D_k^{new}. The value of d_k^{far} can be measured by applying

$$d_k^{\text{far}} = \arg \max_{\forall\, d_l \in D_k^{\text{new}}} \left(dis\left(loc(s_k), d_l\right)\right). \tag{18}$$

Let r_k^{new} be the new sensing radius of s_k after s_k executes three tasks. We have

$$r_k^{\text{new}} = \left(dis\left(loc(s_k), d_k^{\text{far}}\right)\right). \tag{19}$$

By applying (19), sensor s_k can reduce its sensing radius from r_k to r_k^{new} for covering the Voronoi vertex d_k^{far}. When sensor s_k finishes the three tasks, it changes its state from the adjustable node state to the fixed node state.

Although the OR phase can save the energies of the sensors that have larger overlapping region, the sensor with minimal remaining energy, e.g., s_{least}, might not get benefit from the execution of OR phase. This is because that the sensor with minimal remaining energy might not have a big overlapping radius with the other neighboring sensors. In the next phase, the INL phase aims to further prolong the lifetime of sensor s_{least}.

C. Improvement on Network Lifetime Phase

Earlier, the sensor tries to independently reduce its sensing radius, aiming at minimizing the overlapping coverage region. Let s_{least} be the sensor that has the minimal remaining energy compared with its neighbors. Since the lifetime of sensor s_{least} is the local bottleneck of network lifetime, this phase aims to further prolong its lifetime by reducing its sensing radius in a distributed manner. However, an arbitrary reduction on the sensing radius might cause a hole since the sensing radius of each sensor has its contribution in coverage and has been elaborately calculated in previous phases. Different from the OR phase, sensor s_{least} that applies the INL phase should ask for help from its neighboring sensor to cover the new created hole. That is, sensor s_{least} can reduce its sensing radius only if there has some neighboring node that can enlarge its sensing radius for covering the hole created by itself. The following introduces the concept and basic operations designed in this phase.

Initially, each sensor s_i maintains the neighboring information of node $s_j \in N(s_i)$, presented by (r_j, t_j), where t_j denotes the lifetime of sensor s_j. Let $T(s_{\text{least}})$ denote the set of t_j, where $s_j \in N(s_{\text{least}})$. Let $\hat{t}$ denote the least lifetime in set $T(s_{\text{least}})$, which can be measured by applying

$$\hat{t} = \min_{\forall\, t_j \in T(s_{\text{least}})} (t_j). \tag{20}$$

Let $t_{\text{least}}^{\text{final}}$ denote the lifetime of sensor s_{least} after it reduces its sensing radius. To prolong the network lifetime, sensor s_{least} should reduce its sensing radius until the value of $t_{\text{least}}^{\text{final}}$ equals to that of $\hat{t}$. Let e_i^{unit} denote the energy consumption required for sensor s_i in each time unit and $r_{\text{least}}^{\text{final}}$ denote the sensing

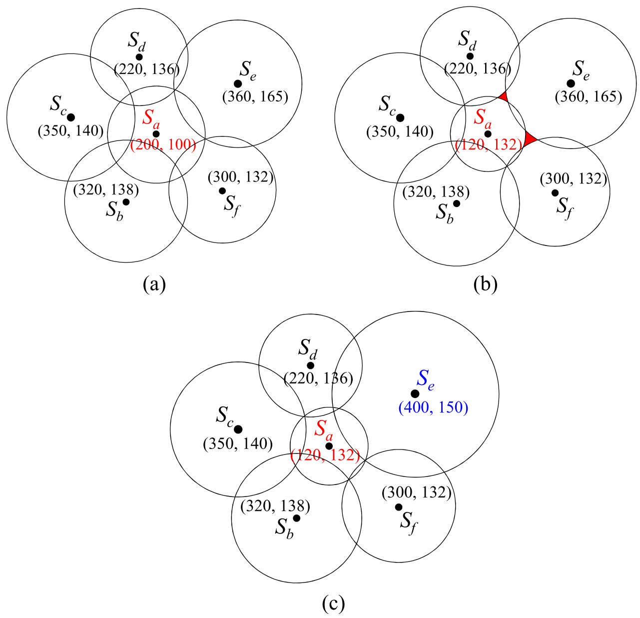

Fig. 12. By applying the INL phase, the network lifetime can be efficiently prolonged. (a) Before executing the INL phase, the network lifetime is 100 time units. (b) By executing the INL phase, the network lifetime can be increased from 100 time units to 132 time units. (c) Sensor s_e functions as the hole healer to cover the hole that is created by sensor s_a.

radius of sensor s_{least} after it reduces its sensing radius. The value of $t_{\text{least}}^{\text{final}}$ can be calculated by applying the following

$$t_{\text{least}}^{\text{final}} = \left(\frac{\gamma \times \left(r_{\text{least}} - r_{\text{least}}^{\text{final}} \right)^2}{e_{\text{least}}^{\text{unit}}} \right) \tag{21}$$

where γ is a constant value.

In the INL phase, if sensor s_{least} reduces its sensing radius, the holes might be created. Consequently, sensor s_{least} further selects one of its neighbors, called hole healer (s^h), to cover the hole. The hole healer enlarges its sensing range aiming to further prolong the network lifetime. Let $t_{\text{sh}}^{\text{final}}$ denote the lifetime of sensor s^h after it adjusts its sensing radius, and let the energy consumption for a time unit of sensor s^h be denoted $e_{\text{sh}}^{\text{unit}}$. Let r_{sh} and $r_{\text{sh}}^{\text{final}}$ denote the sensing radii of sensors s^h and s^h after they adjust their sensing radii, respectively. The following derives the value of $t_{\text{sh}}^{\text{final}}$:

$$t_{\text{sh}}^{\text{final}} = t_{\text{sh}} - \left(\frac{\gamma \times \left(r_{\text{sh}}^{\text{final}} - r_{\text{sh}} \right)^2}{e_{\text{sh}}^{\text{unit}}} \right). \tag{22}$$

The following criterion further specifies the constraints of hole healer. Let $\text{hole}_{\text{least}}$ denote the set of hole areas created by sensor s_{least} and o_i^{final} denote the coverage area of sensor s_i after it adjusts its sensing radius.

Criterion of Hole Healer (s^h)*:* Sensor s_l can be selected as the hole healer of sensor s_{least} if it satisfies the following two criteria.

1) $o_l^{\text{final}} \supseteq \text{hole}_{\text{least}}$
2) $t_l^{\text{final}} \geq t_{\text{least}}$.

Criterion 1 asks sensor s_l which should fully cover the hole. Criterion 2 constrains that the hole healer s^h should not be the bottleneck of the network lifetime. □

Algorithm I: The *WVD-C* phase of sensor s_i.

1. **for** (at the beginning of every period of time T) **do**{
2. /*RPP process*/
3. each sensor s_i calculates the values of r_i and r_j.
$$r_i : r_j = \sqrt{m_i} : \sqrt{m_j} = dis(loc(s_i), p_{ij}) : dis(loc(s_j), p_{ij})$$
4. sensors s_i and s_j adjust their sensing radii to cover the point p_{ij} which is calculated as follows.
$$dis(loc(s_i), p_{ij}) = dis\left(loc(s_i), loc(s_j)\right) \times \frac{\sqrt{m_i}}{\sqrt{m_i}+\sqrt{m_j}} \text{ and}$$
$$dis(loc(s_j), p_{ij}) = dis\left(loc(s_i), loc(s_j)\right) \times \frac{\sqrt{m_j}}{\sqrt{m_i}+\sqrt{m_j}}.$$
5. **if** (*O-Region* exists) **then**{
6. /*REP process */
7. sensor s_i and each of its neighbors s_j, $s_k \in N(s_i)$ calculate the division point p_{ijk}^d and determine the ratio of sensors s_i, s_j, and s_k by applying $\left|\overline{s_i p_{ijk}^d}\right| : \left|\overline{s_j p_{ijk}^d}\right| : \left|\overline{s_k p_{ijk}^d}\right| = \sqrt{m_i} : \sqrt{m_j} : \sqrt{m_k}$.
8. sensor s_i adjusts its sensing radius to cover the division point p_{ijk}^d.
9. **return** c_i;}
10. **else return** c_i;}

Fig. 13. Procedure of WVD-C phase.

The following gives an example to illustrate the operations designed in the INL phase.

As shown in Fig. 12(a), two elements, including parenthesis, present the remaining energy and lifetime of the sensor. Sensor s_a has the least lifetime as compared with its neighbors. It can function as the s_{least} and further reduces its sensing radius. Fig. 12(b) shows that sensor s_a reduces its radius such that its lifetime can be prolonged to 132 time units by applying (20) and (21). However, the holes (marked in red ink) will be created by sensor s_a. To cover the hole, sensor s_a selects sensor s_e to be the hole healer since sensor s_e satisfies two criteria of the hole healer. On the other hand, if there are many hole healer candidates, the sensor that has the maximal lifetime will be selected as the hole healer. Fig. 12(c) shows that sensors s_e enlarges its sensing radius to cover the holes and the network lifetime prolonged from 100 units to 132 units.

IV. Pseudocode of SRA Mechanism

This section presents the algorithm of the proposed SRA protocol. Fig. 13 gives the algorithm of the WVD-C phase. As shown in Fig. 13, lines 1 to 4 determine the weighted Voronoi edge between sensor s_i, and each of its neighbor $s_j \in N(s_i)$ and further constructs the Voronoi cell c_i by applying RPP. However, the O-Region problem might be occurred since each sensor s_i locally decides its weighted Voronoi edge. Therefore, in lines 5 to 9, sensor s_i and each of its neighbor $s_j \in N(s_i)$ cooperatively cover O-Region by applying REP. In line 7, the sensing radius of each sensor can be determined to cover O-Region. After that, each sensor s_i and its neighbors adjust their sensing radii to fully cover O-Region, as shown in line 8. Finally, the WVC c_i can be reconstructed every time period T. On the contrary, if O-Region does not exist, sensor s_i will terminate the WVD-C phase, as depicted in line 10.

Fig. 14 presents the algorithm of OR phase. In lines 2 to 4, sensor s_i checks if it is an adjustable node. If it is not the case, sensor s_i cannot reduce its sensing radius. In case that sensor s_i is an adjustable node, it executes the OR phase. Lines 5–16 illustrate that the adjustable sensor s_i executes the OR phase to replace some vertices from set V_i. In lines 6 and 7, sensor

Algorithm II: The *OR* phase of sensor s_i.

1. /**sensor s_i checks if it is an adjustable node.**/
2. **if** ($v_i^{far} = v_j^{far} = c$) **then**{
3. sensor s_i is fixed node.
4. **break**;}
5. **else** {/**The OR phase**/
6. /**The RFN task**/
7. sensor s_i executes *RFN* task to calculate set D_i^{fixed}.
8. **While** (there exist adjusted nodes){
9. **if** (sensor s_i has the highest value of w_i) **then**{
10. /**The RAN task**/
11. sensor s_i calculates the sets D_i^{adj} and D_i^{new}.
12. /**The SRE task**/
13. sensor s_i covers the vertex $d_i^{far} \in D_i^{adj}$.
14. sensor s_i adjusts its sensing radius from r_i to r_i^{new}.
15. sensor s_i updates the states of its neighbors and itself.
16. **return** r_i^{new};}
17. }}

Fig. 14. Procedure of the OR phase.

Algorithm III: The *INL* phase of sensor s_i.

1. **if** ($s_i \neq s_{least}$) **then**
2. **break**;
3. **else**{/**The INL phase**/
4. sensor s_i calculates the value of t_{least}^{final} and reduces its sensing radius
5. **if** ($hole_{least} \neq \{\emptyset\}$) **then**{
6. **if** (sensor $s_j \in N(s_i)$ satisfies the *Criterion of Hole Healer*) **then**{ $s_j \leftarrow s^h$
7. sensor s^h enlarges its sensing radius and covers the hole}
8. **else break**;
9. **else break**;}}

Fig. 15. Procedure of INL phase of sensor s_i.

s_i executes the RFN task to calculate the set D_i^{fixed}. In lines 9 to 11, if sensor s_i has the highest workload, it can execute the RAN task and then calculate the sets D_i^{adj} and D_i^{new}. Lines 12 to 16 implement the SRE task. Sensor s_i evaluates its sensing radius r_i^{new} to cover the vertex D_i^{new} to update the states of its neighbors and itself.

Fig. 15 further presents the algorithm of the INL phase. Lines 1 and 2 depict that sensor s_i should terminate the INL phase if it cannot play the role of s_{least}. On the contrary, if sensor s_i has the least remaining energy, it can execute the INL phase. In line 4, sensor s_i calculates the value of $t_{\text{least}}^{\text{final}}$ according to (21). To prolong the network lifetime, sensor s_i tries to enlarge its lifetime from $t_{\text{least}}^{\text{final}}$ to $\hat{t}$. However, sensor s_i might create a hole. To cope with this problem, sensor s_i further selects one sensor $s_j \in N(s_i)$ to play the role of s^h for covering the hole, as shown in line 5. In lines 6 and 7, sensor s_i checks sensor s_j, which can be the hole healer or not. If sensor s_j can be the hole healer and cover the hole, sensor s_i can reduce its sensing radius to prolong the network lifetime without creating any hole.

V. Performance Analysis

Here, we aim to analyze the performance improvement of the proposed SRA mechanism against the existing mechanism VD [13] and the optimal approach in terms of the network lifetime. The following first derives the average sensing radius of sensors by applying the compared mechanisms. Then, the lifetimes of a given WSN by applying the proposed SRA, VD, and the optimal mechanisms will be analyzed.

The following calculates the average sensing radius of each sensor by applying the proposed SRA mechanism. Let notation $N(s_i, s_j)$ represent the neighbor relationship of sensors s_i and s_j. The remaining energies of sensor s_i and s_j are m_i and m_j, respectively, where $m_i \leq m_j$. The following defines S_L and S_H that are referred to as the sets of lower energy sensors and higher energy sensors, respectively, i.e.,

$$S_L = \{s_i | N(s_i, s_j) \; \forall \, s_i, s_j \in S\} \tag{23}$$

$$S_H = \{s_j | N(s_i, s_j) \; \forall \, s_i, s_j \in S\} \,. \tag{24}$$

Note that some sensors might be included in both sets S_L and S_H.

The proposed SRA mechanism constructs the WVD based on the remaining energy of each sensor. The following introduces the average energy of sets S_L and S_H. Let M_L and M_H represent the average energy of sets S_L and S_H, respectively. Let $|S_L|$ and $|S_H|$ represent the number of sensors of S_L and S_H, respectively. The following calculate the values of M_L and M_H, respectively:

$$M_L = \frac{1}{|S_L|} \times \sum_{i=1}^{|S_L|} m_i, \text{ where } s_i \in S_L \tag{25}$$

$$M_H = \frac{1}{|S_H|} \times \sum_{j=1}^{|S_H|} m_j, \text{ where } s_j \in S_H. \tag{26}$$

To determine the responsible sensing area of each sensor, we calculate the average distance between sensors s_i and s_j, represented by notation $\text{Dis}(s_i, s_j)$. Let P be the set of (s_i, s_j), where s_i and s_j have the relationship $N(s_i, s_j)$ and $|P|$ denote the number of elements in set P. The average distance, which is called d_{SRA}, of sensors s_i and s_j can be calculated by applying the following:

$$d_{\text{SRA}} = \frac{1}{|P|} \sum_{\forall\,(s_i, s_j) \text{ s.t. } N(s_i, s_j) \in P} \text{Dis}(s_i, s_j). \tag{27}$$

Let notations r and R represent the average sensing radii of sensors $s_i \in S_L$ and $s_j \in S_H$, respectively. Since each sensor applying the SRA scheme will adjust its sensing radius according to its remaining energy, the following holds:

$$\frac{M_H}{M_L} = \frac{kR^2}{kr^2} > 1. \tag{28}$$

Let T^{SRA} represent the network lifetime of the proposed SRA scheme. After determining the average sensing radius of each sensor, the network lifetime can be derived by applying the following:

$$T^{\text{SRA}} = \frac{M_H}{kR^2} = \frac{M_L}{kr^2}. \tag{29}$$

Let $o_{i,j}^{\text{SRA}}$ represent the coverage areas contributed by both s_i and s_j using the SRA mechanism, where $s_i \in S_L$ and $s_j \in S_H$. Similarly, notation $o_{i,j}^{\text{VD}}$ represents the coverage areas contributed by both s_i and s_j using the VD mechanism. To ease the analysis of network lifetimes of SRA and VD mechanisms, we assume that $o_{i,j}^{\mathrm{SRA}}$ equals to $o_{i,j}^{\mathrm{VD}}$. The following discusses how to evaluate the network lifetime of VD. Let the average distance between neighboring sensors s_i, and $s_j \in N(s_i)$ is d_{VD}. Let r_{VD} be the average sensing radius of all sensors after applying the VD mechanism. Based on the assumption $o_{i,j}^{\mathrm{SRA}} = o_{i,j}^{\mathrm{VD}}$, the overall coverage contributed of n sensors by applying SRA and VD mechanisms are identical. The following reflects this argument:

$$n \times \frac{(R^2\pi + r^2\pi)}{2} = n \times r_{\mathrm{VD}}^2 \pi. \tag{30}$$

Therefore, the value of r_{VD} can be further derived, as shown in the following:

$$r_{\mathrm{VD}} = \frac{\sqrt{R^2 + r^2}}{\sqrt{2}}. \tag{31}$$

As a result, the network lifetime T_{VD} by applying VD mechanism can be measured by applying the following:

$$T_{\mathrm{VD}} = \frac{M_L}{k r_{\mathrm{VD}}^2} = \frac{M_L}{k\left(\frac{\sqrt{R^2+r^2}}{\sqrt{2}}\right)^2}. \tag{32}$$

Let the lifetime evaluation index, denoted by $I_{\mathrm{SRA/VD}}$, be the ratio of T^{SRA} to T_{VD}. Substituting (33) into (34), given in the following, the value $I_{\mathrm{SRA/VD}}$ can be derived:

$$R = r\sqrt{\frac{M_H}{M_L}} \tag{33}$$

$$I_{\frac{\mathrm{SRA}}{\mathrm{VD}}} = \frac{T^{\mathrm{SRA}}}{T_{\mathrm{VD}}} = \frac{\left(\frac{M_H}{kR^2}\right)}{\left(\frac{M_L}{k\left(\frac{\sqrt{R^2+r^2}}{\sqrt{2}}\right)^2}\right)} = \frac{\left(\frac{M_H}{M_L}\right)}{2}\left(1 + \frac{r^2}{R^2}\right)$$
$$= \frac{\left(\frac{M_H}{M_L} + 1\right)}{2} \geq 1. \tag{34}$$

The result $I_{\mathrm{SRA/VD}} > 1$, as shown in (34), indicates that the proposed SRA mechanism outperforms the VD scheme in terms of the network lifetime. We notice that the proposed SRA mechanism can provide longer network lifetime when the average energy difference between M_H and M_L is large. For example, when $M_H/M_L = 2$, the network lifetime of the proposed SRA scheme will increases about 50% as compared with the VD scheme.

The following analyzes the network lifetime of the optimal and the proposed SRA mechanisms. Assume that applying the optimal mechanism can obtain an optimal solution where all sensors fully cover the monitoring region with the smallest size of overlapping area. Assume the monitoring region M be a rectangle area $W \times L$. Given a set of n sensors randomly deployed in M, the optimal approach can determine the optimal sensing radius of each sensor. Let r_{opt} denote the average sensing radius of sensors in the optimal solution. The following holds since the monitoring region should be fully covered:

$$n = \frac{WL}{\pi r_{\mathrm{opt}}^2}. \tag{35}$$

The value of r_{opt} can be further calculated by applying the following:

$$r_{\mathrm{opt}} = \sqrt{\frac{WL}{\pi n}}. \tag{36}$$

Let T_{OPT} denote the network lifetime of the optimal solution, which can be evaluated by applying the following:

$$T_{\mathrm{OPT}} = \frac{\sum_{i=1}^{n} m_i}{n} \times \frac{1}{k r_{\mathrm{opt}}^2} = \frac{\pi \sum_{i=1}^{n} m_i}{kWL}. \tag{37}$$

Let the optimal lifetime evaluation index, denoted by $I_{\mathrm{SRA/OPT}}$, be the ratio of T^{SRA} to T_{OPT}. The value $I_{\mathrm{SRA/OPT}}$ can be derived by applying the following:

$$I_{\frac{\mathrm{SRA}}{OPT}} = \frac{T^{\mathrm{SRA}}}{T_{\mathrm{OPT}}} = \frac{\left(\frac{M_H}{kR^2}\right)}{\left(\frac{\pi\sum_{i=1}^{n} m_i}{kWL}\right)}$$
$$= \frac{WLM_H}{\pi R^2 \sum_{i=1}^{n} m_i}, \text{ where } s_i \in S_L \cup S_H. \tag{38}$$

To further observe the value of $I_{\mathrm{SRA/OPT}}$, we assume that the ratio of M_L to M_H is α, where $\alpha \leq 1$. Let notation η represent the size of the covering area outside of the monitoring region M plus the sum of overlapping area sizes between any two sensors by applying the proposed SRA mechanism. To further analyze the performances of the proposed SRA and the optimal mechanisms, we give the overlapping area ratio λ, which can be calculated by η/WL. The following asks that the total covering area by applying the proposed SRA mechanism should fully cover the monitoring region M

$$n \times \frac{(\pi r^2 + \pi R^2)}{2} = (1+\lambda)WL, \text{ where } \lambda \geq 0. \tag{39}$$

Based on (39), the following can be further derived:

$$\frac{n}{2} \times \left(\frac{\pi R^2 M_L}{M_H} + \pi R^2\right) = (1+\lambda)WL$$
$$\Rightarrow \frac{n\pi R^2}{2}(\alpha + 1) = (1+\lambda)WL$$
$$\Rightarrow \frac{WL}{\pi R^2} = \frac{n(\alpha+1)}{2(1+\lambda)}. \tag{40}$$

Let M_{avg} represent the average energy of sensors by applying optimal approach and β denote the ratio of M_{avg} to M_H. Substituting (40) into (38), the value of $I_{\mathrm{SRA/OPT}}$ can be further derived in

$$I_{\frac{\mathrm{SRA}}{\mathrm{OPT}}} = \frac{WL}{\pi R^2} \times \frac{M_H}{\sum_{i=1}^{n} M_i} = \frac{\alpha+1}{2(1+\lambda)} \times \frac{nM_H}{\sum_{i=1}^{n} M_i}$$
$$= \frac{\alpha+1}{2(1+\lambda)} \times \frac{nM_H}{nM_{\mathrm{avg}}} = \frac{\alpha+1}{2\beta(1+\lambda)}. \tag{41}$$

Since the optimal solution has the longest network lifetime, the value of $I_{\mathrm{SRA/OPT}}$ should be smaller than one. The value of $I_{\mathrm{SRA/OPT}}$ approaching to one indicates that the proposed SRA and the optimal approach achieve similar performances. Equation (41) also exhibits that the sensing overhead parameter

TABLE II
SIMULATION PARAMETERS

Parameter	Value
Size of monitoring region	1500 *1500m^2
Number of sensors	500 ~ 1000 nodes
Initial energy of each sensor	10,000 J
Packet transmission cost	0.075 J/s
Packet reception cost	0.030 J/s
Idle cost	0.025 J/s
Data report time t	3 ~ 12 hours

λ and the energy parameters α and β are key factors that affect the performance of the proposed SRA approach. More specifically, a large value of α and smaller values of λ and β will enlarge the value of $I_{\mathrm{SRA/OPT}}$ and, hence, improve the performance of the proposed SRA mechanism. The following further presents the observations based on (41). First, since the values of α and β will be determined before initiating the SRA approach, both two values represent the given energy conditions in the investigated environment. In fact, the value of α is less than or equal to β by the definitions. That is, we have $\alpha \leq \beta \leq 1$.

Let δ be a constant satisfying the condition $\alpha \geq \delta\beta$. That is, $M_L \geq \delta M_{\mathrm{avg}}$. Equation (42) can be further derived from (41). This also indicates that the optimal lifetime evaluation index $I_{\mathrm{SRA/OPT}}$ guarantees a lower bounded and is controlled by the values of β and λ, as shown in the following:

$$I_{\frac{\mathrm{SRA}}{\mathrm{OPT}}} \geq \frac{\delta\beta}{2\beta(1+\lambda)} + \frac{1}{2\beta(1+\lambda)} = \frac{1}{2(1+\lambda)}\left(\delta + \frac{1}{\beta}\right). \quad (42)$$

Second, in (42), a smaller value of β helps enlarge the value of $I_{\mathrm{SRA/OPT}}$. Therefore, the number of sensors with low energy is high. In the case, applying the SRA approach is able to balance the sensing radius with the neighboring sensors whose energy is relative high. Hence, SRA and optimal approaches achieve similar performances. Finally, the sensing radius of each sensor is adjusted by the proposed SRA mechanism in a distributed manner (according to the energies of neighboring sensors). Compared with the centralized optimal approach, the proposed SRA mechanism has more sensing overheads. In (42), a smaller value of λ helps enlarge the value of $I_{\mathrm{SRA/OPT}}$ and hence improve the performance of the proposed SRA approach.

According to (34) and (42), we have the fact that the performance of the proposed SRA mechanism is better than that of the VD mechanism but is worse than that of the optimal approach. This fact also can be verified by the experiment as shown in Fig. 20.

VI. PERFORMANCE EVALUATION

Here, the performance improvement of the proposed SRA mechanism is examined against the existing approaches in [13] and [16], which are referred to as VD and DT, respectively. Table II gives the parameters used in the simulation. Each simulation result is obtained from the average of 100 independent runs, and the 95% confidence interval is always smaller than 5% of the reported values.

Moreover, the sensing cost model [22] is used in this paper.

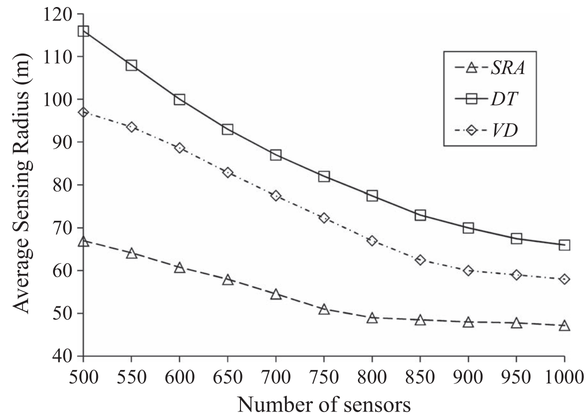

Fig. 16. Comparison of three coverage mechanisms in terms of the average sensing radius.

Sensing Cost Model: The relationship between sensing radius and energy consumption of a sensor depends on the characteristics of the sensing device. In [22], the sensing power law function H of a sensor node is modeled as $H(r_i) = H_0 r_i^x$, where r_i denotes the sensing radius of sensor s_i, and x can be considered decay exponent for the sensed signal and would depend upon the sensor components. The value of x, normally ranging from 2 to 4 [23], will practically impact the energy consumption of a sensor node. Most existing works [24], [25] use $x = 2$ as their sensing models when measuring the energy consumption for sensing operation. In the proposed SRA mechanism, the sensing cost is also modeled as $e_i = kr_i^2$. To investigate the impact of x on the network lifetime of the proposed SRA mechanism, an additional experiment that changes the value of x ranging from 2 to 4 is shown in Fig. 19.

Fig. 16 depicts the performance comparison of three mechanisms in terms of the average sensing radius. Generally, the average sensing radius decreases with the number of sensors. By applying the existing DT scheme, each sensor adjusts its sensing radius based on its remaining energy. However, the DT mechanism leads to the energy-unbalanced problem, as shown in Fig. 16. In addition, the sensors located at the boundary will enlarge its sensing radius, increasing the large average sensing radius. On the other hand, the VD mechanism calculates the sensing radius of each sensor based on the bisector Voronoi edge. However, the VD mechanism does not reduce the overlapping region; hence, it has larger average sensing radius than the proposed SRA mechanism. By applying the proposed SRA mechanism, any node located at the boundary of the monitoring area treats the boundary as the weighted Voronoi edge of its cell in WVD-C phase, achieving the purpose of full coverage. As shown in Fig. 16, the SRA mechanism has better performance than DT and VD mechanisms in terms of the average sensing radius.

Fig. 17 compares the proposed SRA mechanism with VD and DT approaches in terms of the network lifetime. The network lifetime is measured by the time interval starting from the time that sensors have been deployed to the time that any coverage hole appears. The number of sensors is controlled ranging from 500 to 1000. As shown in Fig. 17, since the VD approach does not consider the factor of energy balance and DT approach

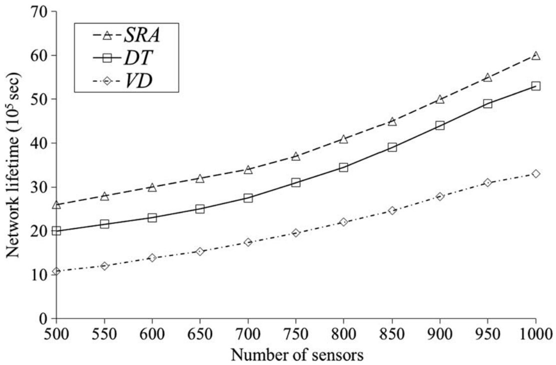

Fig. 17. Impact of the number of sensors on the network lifetime.

has the energy-unbalanced problem, the network lifetimes of VD and DT mechanisms are shorter than that of SRA mechanism. On the contrary, the proposed SRA mechanism applies WVD-C phase to determine the responsible sensing region of each sensor based on the remaining energy. Moreover, the proposed SRA mechanism further prolongs the network lifetime by applying OR and INL phases. Consequently, the proposed SRA mechanism outperforms VD and DT mechanisms in terms of the network lifetime in all cases.

The proposed SRA mechanism aims to prolong the network lifetime by constructing WVD where each sensor's responsible region is determined by the differences of remaining energy between each sensor and its neighbors. Let $m_{i,j}^{\text{diff}}$ denote the total remaining energy difference between sensor s_i and all its neighbors $s_j \in N(s_i)$. We have

$$m_{i,j}^{\text{diff}} = \sum_{j=1}^{n(s_i)} |m_j - m_i| \; \forall s_j \in N(s_i) \tag{43}$$

where $n(s_i)$ denotes the number of neighbors of s_i. Let e_{total} denote the initial energy of the sensor. The NLI denotes the normalized energy difference an it is controlled between 0 and 1, as shown in

$$\text{NLI} = \frac{m_{i,j}^{\text{diff}}}{e_{\text{total}} \times n(s_i)}. \tag{44}$$

A lower value of NLI indicates that the remaining energies of any two sensors are better balanced. It also implies that the given WSN has longer network lifetime. Fig. 18 further investigates the value of NLI by varying the value of initial energy difference ranging from 0.1 to 1.0. The initial energy difference, denoted by IED, is referred to as the average difference of initial energies between any pair of sensors. In Fig. 18, the curve of VD is sharply increased since each sensor did not adjust its sensing radius. That is, each sensor s_i constructs the Voronoi edge according to the distance between s_i and its Voronoi neighbor $s_j \in N(s_i)$. On the other hand, the curve of the DT mechanism is also increased since each sensor does not reduce the overlapping area, leading to unnecessary energy consumption. The proposed SRA approach applies the WVD-C phase and hence each sensor can reconstruct its WVC periodically. Compared with the DT mechanism, the SRA mechanism has smaller value of NLI, which indicates that SRA outperforms DT in terms of the energy balance.

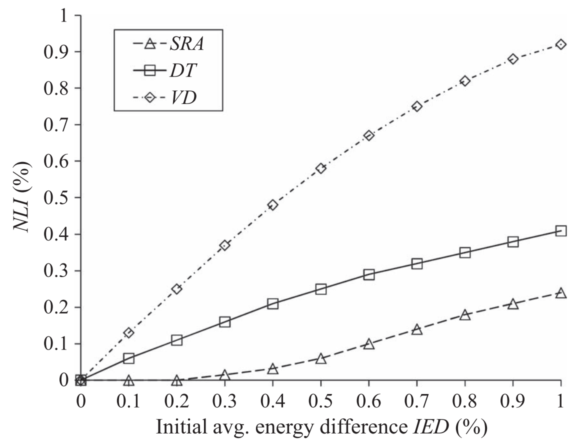

Fig. 18. Value of NLI versus the initial energy difference.

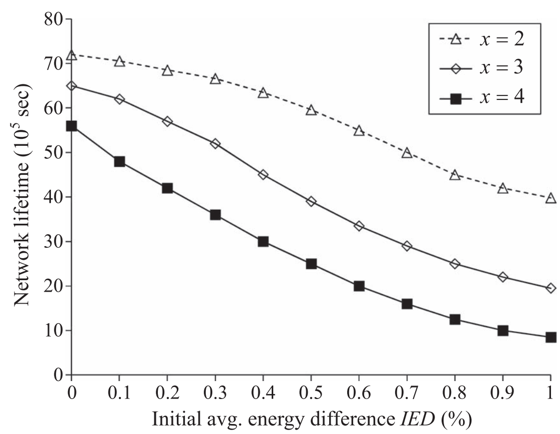

Fig. 19. Impact of different values of x on the network lifetime by varying the initial energy difference.

Fig. 19 shows the impact of different values of x on the network lifetime by varying the value of *IED* in the SRA mechanism. In general, all curves of three values are decreased with the value of IED. As shown in Fig. 19, the value of x has strong effects on the network lifetime. The performance of $x = 2$ outperforms those of $x = 3$ and $x = 4$ nearly 2.3 and 4.7 times, respectively, when the value of IED approaches to 1.

In addition to analyzing the performance comparison of the optimal and the proposed SRA mechanisms, an additional experiment, as found in Fig. 20, further compares the performances of the optimal and the proposed SRA mechanisms. In Fig. 20, the proposed SRA mechanism is compared with the optimal approach (denoted by *Optimal*) and the existing approaches, including VD [13] and DT [16] mechanisms. The optimal solutions are obtained by exhaustive algorithm. In the environment, the value of IED is varied, ranging from 0 to 1. In general, the network lifetime of all approaches are decreased with the value of IED. Since the optimal approach considers all solutions in a centralized manner, each sensor can minimize its sensing radius while the full coverage constraint can be satisfied. Therefore, the optimal approach has the longest network lifetime. The DT and SRA approaches have better performance than VD mechanism since both of them construct the responsible region of each sensor according to the remaining

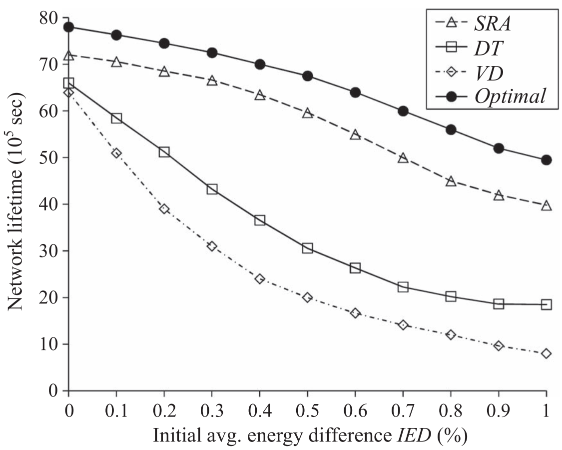

Fig. 20. The comparison of four mechanisms in terms of the network lifetime by varying the initial energy difference.

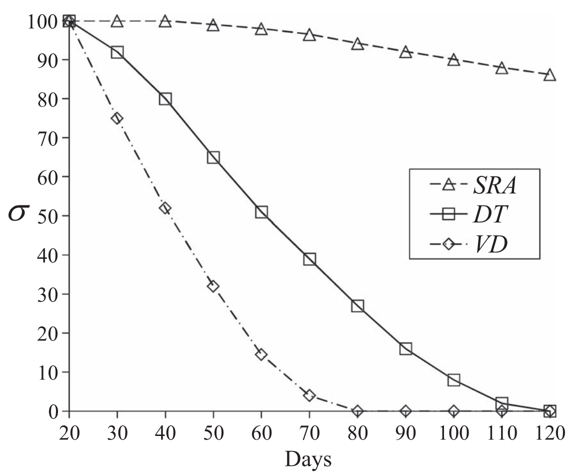

Fig. 21. Comparison of three mechanisms in terms of the coverage ratio σ.

energy. However, the DT mechanism does not further reduce the overlapping region, leading to unnecessary energy consumption. As shown in Fig. 20, the proposed SRA mechanism outperforms DT mechanism in terms of the network lifetime. This occurs because that the proposed SRA mechanism applies OR and INL phases, aiming at prolonging the network lifetime. Accordingly, the proposed SRA mechanism outperforms DT and VD approaches in terms of the network lifetime in all cases.

Fig. 21 further measures the monitoring quality when the coverage hole appears. It compares the three coverage mechanisms in terms of the coverage ratio σ. Let A_{cover} denote the area size covered by sensors in M. The coverage ratio σ can be represented by

$$\sigma = \frac{A_{\text{cover}}}{WL}. \tag{45}$$

The three approaches have 100% coverage ratio for 20 days starting from the day that the three approaches are applied. Since the VD mechanism does not consider the factor of energy balance, the curve of VD drops earlier than that of the other two compared schemes. The DT approach considers the energies of all sensors. However, some sensors with higher remaining

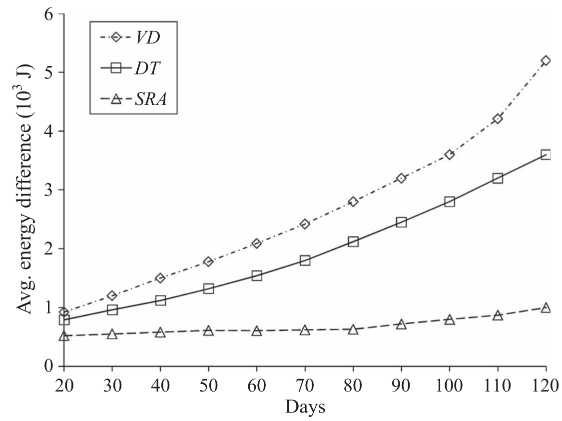

Fig. 22. Comparison of SRA, DT, and VD mechanisms in terms of the average energy difference.

energies might still fail because the sensors did not reduce the overlapping area. Hence, the performance of the DT approach is between that of VD and SRA schemes. In SRA mechanism, each sensor initially determines its own responsible sensing region by using RPP and REP (if any). Then, the adjustable node executes the OR phase to minimize the coverage redundancy. Consequently, the energy consumptions of all sensors can be balanced, and the coverage redundancy of any two sensors can be minimized. Thus, the curve of SRA mechanism keeps a constant shape. In general, the proposed SRA mechanism outperforms the VD and DT approaches in terms of the coverage ratio in all cases.

Fig. 22 compares SRA, VD, and DT approaches in terms of the average energy difference. The experimental results are observed during 100 days. We randomly choose two sensors and calculate the average energy difference between them. Generally, the average energy differences of three approaches are increased with the elapsed days. The main reason is that sensors have different sensing radius to cover their own responsible cells. The VD mechanism does not take into consideration the remaining energy of each sensor; thus, the average energy difference is higher than the other two mechanisms. By applying the DT mechanism, each sensor constructs its responsible region according to its remaining energy; thus, the performance of the DT scheme is better than that of the VD mechanism. The curve of the SRA mechanism grows slower than those of DT and VD mechanisms. The major reason is that the SRA mechanism takes energy balance into consideration; hence, each sensor determines its own responsible sensing region based on the remaining energy. Overall, the proposed SRA mechanism has better performance than the other two schemes in terms of the average energy difference.

The proposed SRA approach mainly consists of three phases, including the WVD-C, OR, and INL phases. Fig. 23 investigates the impact of each phase on the overlapping sensing region by varying the number of sensors, ranging from 500 to 1000. The Policy I only constructs WVD without reduction of overlapping region of each sensor. The Policy I + II additionally involves the operations of OR phase, which efficiently reduces the overlapping region of the adjustable sensors. Recall the notation y_{ij} denotes the size of intersection region of sensing

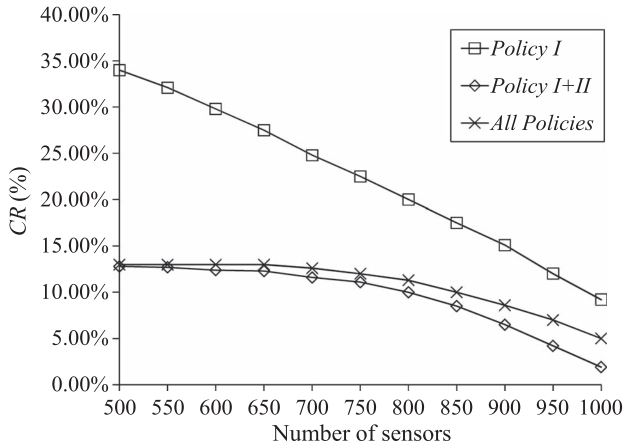

Fig. 23. Comparison of the overlapping ratio that indicates the contribution of each phase designed in the SRA mechanism.

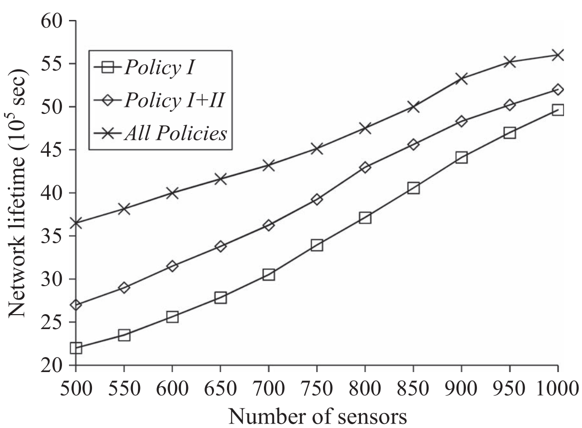

Fig. 24. Impact of the number of sensors on the network lifetime by applying difference policies.

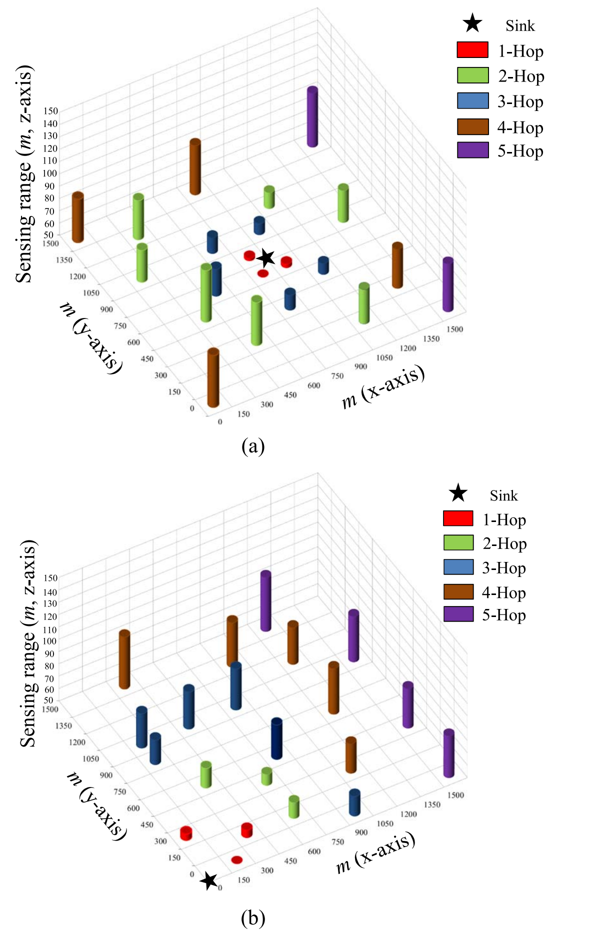

Fig. 25. Impact of the location of sink on the sensor's sensing radius. (a) Sink is located at the center of M. (b) Sink is located at the corner of M.

regions of sensors s_i and s_j. Let CR denote the overlapping ratio of M, which can be evaluated by the formula

$$\mathrm{CR} = \sum_{i=1}^{n-1} \sum_{j=i+1}^{n} \left(\frac{y_{ij}}{o_i + o_j} \right) \forall\, s_j \in N(s_i). \tag{46}$$

The value of CR is always smaller than one because that the overlapping region of s_i and s_j cannot be larger than the summation of their sensing regions. As shown in Fig. 23, the overlapping ratios of the three phases likely maintain constant values when the number of sensors is increased. Without reducing of overlapping region, the constructed WVD by Policy I will induce the larger overlapping area than other two phases. Policy I + II has the smallest overlapping ratio than the others since Policy I + II further reduces the overlapping region in OR phase. The *All policies* additionally executes the INL phase that aims to prolong the network lifetime. Therefore, the performance of *All policies* is lower than that of Policy I + II.

Fig. 24 further measures the network lifetime by varying the number of sensors ranging from 500 to 1000. Mostly, the curves of all polices obviously increase with the number of sensors. The Policy I constructs the WVD without taking into consideration the overlapping region. As the result, Policy I has the shortest network lifetime. On the other hand, Policy I + II executes the OR phase aiming to reduce the overlapping region for further prolonging the network lifetime. However, it cannot prolong the lifetime of the sensor, which has the least lifetime. As a result, the network lifetime of Policy I + II is shorter than that of the *All-policies*. In Fig. 24, the *All policies* has the longest network lifetime since it additionally applies the INL phase. Consequently, the *All-policies* outperforms the Policy I and Policy I + II approaches in terms of the network lifetime.

Fig. 25 observes the relationship of location and sensing radius of each sensor by applying the proposed SRA mechanism. The x-axis and y-axis, ranging from 0 m to 1500 m, represent the coordinates of M. The z-axis denotes the required average sensing radius of sensors such that the monitoring region can be fully covered. The location of sink node, as marked in star symbol, is set at the center or the corner of M. We selectively choose some sensors and investigate their average sensing radii. In Fig. 25(a), the location of sink is set at the center of M. The sensors which are one-hop neighbors of the sink node have small sensing radius (marked in red ink). The major reason is that these sensors have to relay a large number of data to sink, leading to high energy consumption. To balance their energy consumption, their sensing radii are smaller than the two-hop neighbors of the sink node. On the contrary, the sensor with large sensing radius (marked in purple ink) indicates that it has lower energy consumption. Hence, it can contribute a larger sensing radius to achieve both purposes of the energy balance and full coverage. In Fig. 25(b), the location of sink is set at corner of M. The results are similar to Fig. 25(a). Overall, the proposed SRA mechanism adjusts the sensing radius of each sensor to prolong the network lifetime.

VII. Conclusion

This paper has considered the area coverage problem for a given WSN whereby each sensor has variable sensing radius. There are two major objectives in this paper. One is to balance the lifetimes of all sensors, and the other is to minimize the intersection area of any two neighboring nodes. To balance the lifetimes of all sensors, each sensor applies the proposed SRA mechanism to locally adjust its sensing radius based on its own and its neighbors' current remaining energies. This paper has initially proposed a WVD that is constructed by each sensor. Based on the constructed WVD, each sensor locally adjusts its sensing range so that the remaining energies of its neighbors and itself can be balanced. Furthermore, to prolong the network lifetime of the given WSN, the sensor with the largest remaining energy can locally enlarge its sensing range to improve the lifetime of the neighboring sensor, which has the minimal remaining energy. In the performance study, we compare the proposed SRA with the existing VD and DT approaches. The proposed SRA significantly outperforms DT and VD mechanisms in terms of network lifetime, coverage ratio, and average energy difference.

References

[1] M. Krysander and E. Frisk, "Sensor placement for fault diagnosis," *IEEE Trans. Syst., Man, Cybern. A, Syst., Humans*, vol. 38, no. 6, pp. 1398–1410, Nov. 2008.

[2] M. Li, W. Cheng, K. Liu, Y. He, X. Y. Li, and X. Liao , "Sweep coverage with mobile sensors," *IEEE Trans. Mobile Comput.*, vol. 10, no. 11, pp. 1534–1545, Nov. 2011.

[3] O. M. Younis, M. M. Krunz, and S. Ramasubramanian, "ROC: Resilient online coverage for surveillance applications," *IEEE/ACM Trans. Netw.*, vol. 19, no. 1, pp. 251–264, Feb. 2011.

[4] C. Y. Chang, C. Y. Lin, C. T. Chang, and W. C. Chu, "An energy-balanced swept-coverage mechanism for mobile WSNs," *J. Wireless Netw.*, vol. 19, no. 5, pp. 871–889, Jul. 2013.

[5] C. Liu, K. Wu, Y. Xiao, and B. Sun, "Random coverage with guaranteed connectivity: Joint scheduling for wireless sensor networks," *IEEE Trans. Parallel Distrib. Syst.*, vol. 17, no. 6, pp. 562–575, Jun. 2006.

[6] Z. Yun, X. Bai, D. Xuan, T. H. Lai, and W. Jia, "Optimal deployment patterns for full coverage and k-connectivity ($k \leq 6$) wireless sensor networks," *IEEE/ACM Trans. Netw.*, vol. 18, no. 3, pp. 934–947, Jun. 2010.

[7] Q. Yang, S. He, J. Li, J. Chen, and Y. Sun, "Energy-efficient probabilistic area coverage in wireless sensor networks," *IEEE Trans. Veh. Technol.*, vol. 64, no. 1, pp. 367–377, Jan. 2015.

[8] A. Chen, S. Kumor, and T. H. Lai, "Designing localized algorithms for barrier coverage," in *Proc. ACM MobiCom*, Montreal, QC, Canada, Sep. 2007, pp. 63–74.

[9] C. Y. Chang, C. Y. Hsiao, and C. T. Chang, "The k-barrier coverage mechanism in wireless visual sensor networks," in *Proc. IEEE WCNC*, Shanghai, China, Apr. 2012, pp. 2318–2322.

[10] W. Wang, V. Srinivasan, B. Wang, and K. C. Chua, "Coverage for target localization in wireless sensor networks," *IEEE Trans. Wireless Commun.*, vol. 7, no. 2, pp. 667–676, Feb. 2008.

[11] C. Y. Chang, C. Y. Lin, C. Y. Hsieh, and Y. J. Ho, "Patrolling mechanisms for disconnected targets in wireless mobile data mules networks," in *Proc. ICPP*, Taipei, Taiwan, Sep. 2011, pp. 93–98.

[12] Z. Lu, W. W. Li, and M. Pan, "Maximum lifetime scheduling for target coverage and data collection in wireless sensor networks," *IEEE Trans. Veh. Technol.*, vol. 64, no. 2, pp. 714–727, Feb. 2015.

[13] B. A. Bash and P. J. Desnoyers, "Exact distributed voronoi cell computation in sensor networks," in *Proc. IPSN*, Cambridge, MA, USA, Apr. 2007, pp. 236–243.

[14] N. Bartolini, T. Calamoneri, T. L. Porta, C. Petrioli, and S. Silvestri, "Sensor Activation and Radius Adaptation (SARA) in heterogeneous sensor networks," *ACM Trans. Sensor Netw.*, vol. 8, no. 3, p. 24, Jul. 2012.

[15] J. Wang and S. Medidi, "Energy efficient coverage with variable sensing radii in wireless sensor networks," in *Proc. IEEE WiMob*, White Plains, NY, USA, Oct. 2007, p. 61.

[16] C. T. Vu and Y. Li, "Delaunay-triangulation based complete coverage in wireless sensor networks," in *Proc. IEEE PerCom*, Galveston, TX, USA, Mar. 2009, pp. 1–5.

[17] J. P. Sheu, W. K. Hu, and J. C. Lin, "Distributed localization scheme for mobile sensor networks," *IEEE Trans. Mobile Comput.*, vol. 9, no. 4, pp. 516–526, Apr. 2010.

[18] B. Xiao, L. Chen, Q. Xiao, and M. Li, "Reliable anchor-based sensor localization in irregular areas," *IEEE Trans. Mobile Comput.*, vol. 9, no. 1, pp. 60–72, Jan. 2009.

[19] B. Xiao, H. Chen, and S. Zhou, "Distributed localization using a moving beacon in wireless sensor networks," *IEEE Trans. Parallel Distrib. Syst.*, vol. 19, no. 5, pp. 587–600, May 2008.

[20] K. F. Ssu, C. H. Ou, and H. C. Jiau, "Localization with mobile anchor points in wireless sensor networks," *IEEE Trans. Veh. Technol.*, vol. 54, no. 3, pp. 1187–1197, May 2005.

[21] R. Jain, D. Chiu, and W. Hawe, "A quantitative measure of fairness and discrimination for resource allocation in shared computer systems," Digit. Equip. Corp., Hudson, MA, USA, DEC-TR-301, Sep. 1984.

[22] S. Pattem, S. Poduri, and B. Krishnamachari, "Energy-quality tradeoffs for target tracking in wireless sensor networks," in *Proc. IPSN*, Palo Alto, CA, USA, Apr. 2003, pp. 32–46.

[23] P. Wan, G. Calinescu, X. Li, and O. Frieder, "Minimum-energy broadcast routing in static ad hoc wireless networks," in *Proc. IEEE INFOCOM*, Anchorage, AK, USA, Apr. 2001, pp. 1162–1171.

[24] M. Cardei, J. Wu, M. Lu, and M. Pervaiz, "Maximum network lifetime in wireless sensor networks with adjustable sensing ranges," in *Proc. IEEE WiMob*, Montreal, QC, Canada, Aug. 2005, pp. 438–445.

[25] M. Cardei, M. Thai, Y. Li, and W. Wu, "Energy-efficient target coverage in wireless sensor networks," in *Proc. IEEE INFOCOM*, Miami, FL, USA, Mar. 2005, pp. 1976–1984.

Chao-Tsun Chang (M'12) received the Ph.D. degree in computer science and information engineering from National Central University, Taoyuan, Taiwan, in 2006.

He is currently an Associate Professor with the Department of Information Management, Hsiuping University of Science and Technology, Taichung, Taiwan. In the past ten years, he has directed 12 research projects, including five National Science Council projects and seven information system developments. His current research interests include ad hoc wireless networks, wireless sensor networks, Bluetooth radio networks, and mobile computing.

Dr. Chang is a member of the IEEE Computer and Communication Societies.

Chih-Yung Chang (M'05) received the Ph.D. degree in computer science and information engineering from National Central University, Taoyuan, Taiwan, in 1995.

He is currently a Full Professor with the Department of Computer Science and Information Engineering, Tamkang University, New Taipei City, Taiwan. His current research interests include Internet of Things, wireless sensor networks, ad hoc wireless networks, and Long-Term Evolution broadband technologies.

Dr. Chang has served as an Associate Guest Editor for several SCI-indexed journals, including the *Journal of Internet Technology* from 2004 to 2008, the *Journal of Information Science and Engineering* in 2008, the *Telecommunication Systems* in 2010, the *IET Communications* in 2011, the *International Journal of Ad Hoc and Ubiquitous Computing* from 2011 to 2016, and the *International Journal of Distributed Sensor Networks* from 2012 to 2014.

Shenghui Zhao received the Ph.D. degree from Southeast University, Nanjing, China, in 2013.

She is currently a Professor with the School of Computer and Information Engineering and the Head of the Research Group of Cloud Computing and Big Data, Chuzhou University, Chuzhou, China. Her current research interests include cloud computing, big data, and Internet of Things.

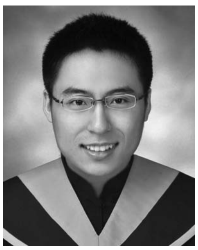

Jian-Cheng Chen received the B.S. and M.S. degrees in computer science and information engineering, in 2012 and 2013, respectively, from Tamkang University, New Taipei City, Taiwan where he is currently working toward the Ph.D. degree.

His current research interests include Internet of Things, cyber–physical systems, wireless sensor networks, ad hoc wireless networks, and Long-Term Evolution Advanced broadband technologies.

Mr. Chen has received several scholarship grants in Taiwan and has participated in various projects related to the above areas.

Tzu-Lin Wang received the B.S. and M.S. degrees in computer science and information engineering from Aletheia University, New Taipei City, Taiwan, in 2007 and 2009, respectively, and the Ph.D. degree from Tamkang University, New Taipei City, in 2014.

She is currently with the Industrial Technology Research Institute, Hsinchu, Taiwan. Her current research interests include wireless sensor networks, ad hoc wireless networks, mobile/wireless computing, software-defined networking, and OpenStack.